Supplemental Information

Ionic conductivity, viscosity, and self-diffusion coefficients of novel imidazole salts for lithium-ion battery electrolytes

Anna Szczęsna-Chrzan[a,*], Monika Vogler[b,c,*], Peng Yan[d,*], Grażyna Zofia Żukowska[a], Christian Wölke[d], Agnieszka Ostrowska[a], Sara Szymańska[a], Marek Marcinek[a], Martin Winter[d], Isidora Cekic-Laskovic[d,†], Władysław Wieczorek[a,†], and Helge S. Stein[b,c,†]

[a.] *Faculty of Chemistry, Warsaw University of Technology, Noakowskiego 3, Warsaw 00-664, Poland*
[b.] *Helmholtz Institute Ulm, Applied Electrochemistry, Helmholtzstr. 11, 89081 Ulm, Germany*
[c.] *Karlsruhe Institute of Technology, Institute of Physical Chemistry, Fritz-Haber-Weg 2, 76131 Karlsruhe, Germany*
[d.] *Helmholtz Institute Münster (IEK-12), Forschungszentrum Jülich GmbH, Corrensstraße 46, 48149 Münster, Germany*
** AS, MV and PY contributed equally*

1 Electrolyte formulation and conducted measurements

This section presents a table summarizing the electrolyte formulations used in this study, their preparation procedure and the selected measurements, for which they were used.

The procedures applied to formulate the electrolytes used in our study are described in the following. Commercially available 1 M $LiPF_6$ in EC:EMC (3:7 by weight) is used as a reference in EIS and viscosimetry since it is an established industry standard and to mitigate deviations between the references at different laboratories. For NMR, a 1.5 M $LiPF_6$ solution is diluted by pre-mixed EC:EMC (3:7 by weight) to ensure the same treatment of all electrolytes including the reference.

A. Automated gravimetric dispensing of all components using the robotic system described in[1].
B. Manual formulation of stock solutions by gravimetric dosing followed by manual volumetric dosing of the stock solutions controlled by weighing after the addition of each stock solution.

Table SI-1: Overview of the electrolytes used in this study, the respective formulation method and performed measurements. All the electrolyte formulations contain EC:EMC (3:7 by weight) as a solvent mixture. The electrolyte formulation labels report the nominal concentration of the conducting salt in $mol \cdot L^{-1}$ and the respective conducting salt.

Electrolyte formulation label	Formulation method	Measurements
1 M $LiPF_6$ (benchmark)	purchased	EIS, viscosimetry
1 M $LiPF_6$ (benchmark)	B	NMR
0.05 M LiTDI	A	EIS, viscosimetry
0.05 M LiPDI	A	EIS, viscosimetry
0.05 M LiHDI	A	EIS, viscosimetry
0.6 M LiTDI	A	EIS, viscosimetry
0.6 M LiPDI	A	EIS, viscosimetry
0.6 M LiHDI	A	EIS, viscosimetry
1 M LiTDI	A	EIS, viscosimetry
1 M LiPDI	A	EIS, viscosimetry
1 M LiHDI	A	EIS, viscosimetry
0.05 M LiTDI	B	NMR
0.05 M LiPDI	B	NMR
0.05 M LiHDI	B	NMR

0.1 M LiTDI	B	NMR
0.1 M LiPDI	B	NMR
0.1 M LiHDI	B	NMR
0.3 M LiTDI	B	NMR
0.3 M LiPDI	B	NMR
0.3 M LiHDI	B	NMR
0.6 M LiTDI	B	NMR
0.6 M LiPDI	B	NMR
0.6 M LiHDI	B	NMR
1 M LiTDI	B	NMR
1 M LiPDI	B	NMR
1 M LiHDI	B	NMR

2 Deviation from theoretical behavior in J-PGSE

Figure SI-1 shows exemplarily the intensities of the two signals of the PF_6^- doublet in the ^{19}F J-PGSE measurement plotted versus the gradient strength for the electrolyte containing 0.3 M $LiPF_6$ in EC:EMC (3:7 by weight). It can be seen, that the initial intensity in the absence of a gradient is not the maximum intensity for both of the signals. This is observed for several other single salt electrolytes in this study as well.

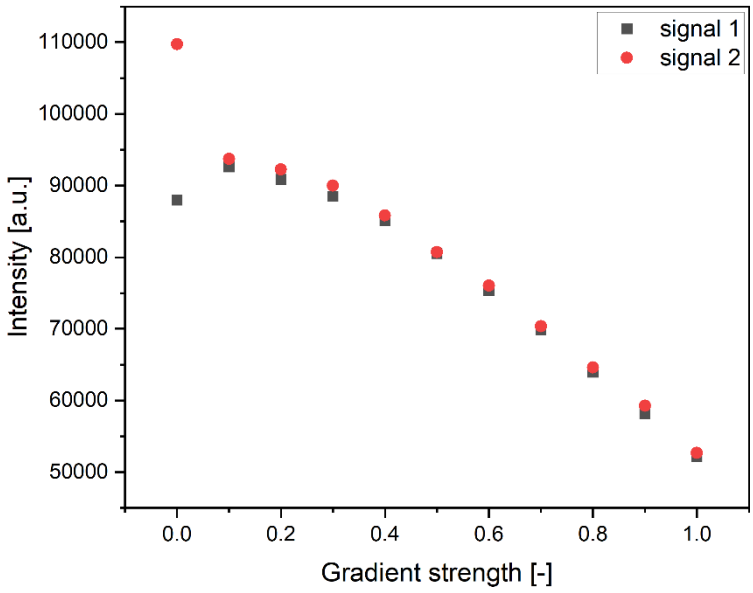

Figure SI-1: The intensity of the two signals of the PF_6^- doublet in the fluorine J-PGSE measurement plotted *vs.* the gradient strength for the electrolyte containing 0.3 M $LiPF_6$ in EC:EMC (3:7 by weight). The maximum intensity is observed at zero gradient only for one of the two signals.

3 Analysis of the Walden plot

Deviations from the ideal KCl line determined from the Walden plots presented in the manuscript are presented in Table SI-2 for 20 °C and Table SI-3 for 40 °C, respectively.

Table SI-2: Deviations from the ideal KCl line at 20 °C for electrolyte formulations containing considered conducting salts in EC:EMC (3:7 by weight). The electrolyte formulations are labelled as in Table SI-1.

20 °C			
Electrolyte formulation label	**$\log(\sigma_m)_{ideal}$ [log(S · cm² · mol-1)]**	**$\log(\sigma_m)_{actual}$ [log(S · cm² · mol^{-1})]**	**Vertical deviation from ideal KCl [log(S · cm² · mol^{-1})]**
0.05 M LiTDI	1.92526	1.27784	-0.65
0.05 M LiPDI	1.92893	1.28375	-0.65
0.05 M LiHDI	1.93449	1.27323	-0.66
0.6 M LiTDI	1.72688	0.81057	-0.92
0.6 M LiPDI	1.67117	0.87322	-0.80
0.6 M LiHDI	1.66298	0.84126	-0.82
1 M LiTDI	1.51412	0.59737	-0.92
1 M LiPDI	1.45192	0.61784	-0.83
1 M LiHDI	1.41355	0.56419	-0.85
1 M $LiPF_6$	1.44434	0.89387	-0.55

Table SI-3: Deviations from the ideal KCl line at 40 °C for electrolyte formulations containing considered conducting salts in EC:EMC (3:7 by weight). The electrolyte formulations are labelled as Table SI-1.

40 °C			
Electrolyte formulation label	**$\log(\sigma_m)_{ideal}$ [log(S · cm² · mol^{-1})]**	**$\log(\sigma_m)_{actual}$ [log(S · cm² · mol^{-1})]**	**Vertical deviation from ideal KCl [log(S · cm² · mol^{-1})]**
0.05 M LiTDI	2.05308	1.39655	-0.66
0.05 M LiPDI	2.05552	1.39967	-0.66
0.05 M LiHDI	2.0625	1.38952	-0.67
0.6 M LiTDI	1.87345	0.95545	-0.92
0.6 M LiPDI	1.81508	1.01939	-0.80
0.6 M LiHDI	1.81364	0.98975	-0.82
1 M LiTDI	1.68715	0.76708	-0.92
1 M LiPDI	1.62357	0.78661	-0.84
1 M LiHDI	1.59295	0.74092	-0.85
1 M $LiPF_6$	1.63209	1.03197	-0.60

The slopes determined from the Walden plots for the individual electrolyte formulations investigated in this study are presented in Table SI-4

Table SI-4: Slopes for all considered electrolyte formulations as obtained from the Walden plots. All electrolyte formulations contain EC:EMC (3:7 by weight) as the solvent mixture.

Electrolyte formulation label	**Slope [log(S cm² mol^{-1}) log(P^{-1})]**
0.05 M LiTDI	0.97
0.05 M LiPDI	0.94
0.05 M LiHDI	0.93
0.6 M LiTDI	1.00
0.6 M LiPDI	0.98
0.6 M LiHDI	0.96
1 M LiTDI	0.98
1 M LiPDI	0.95
1 M LiHDI	0.95
1 M $LiPF_6$	0.80

4 NMR-spectra of the salts under investigation

This section presents the NMR spectra obtained for the salts under investigation. The ^{1}H, ^{19}F, and ^{13}C NMR spectra were recorded in CD_3CN, with a Varian VNMRS spectrometer, operating at 500 MHz. The ^{19}F and ^{13}C NMR spectra confirm the structures of the lithium salts. The ^{7}Li NMR spectra were recorded for a concentration of 0.63 M salt in EC:EMC (3:7 by weight) without a deuterated solvent using LiCl in D_2O as an external reference.

4.1 ^{1}H-NMR

4.1.1 LiTDI

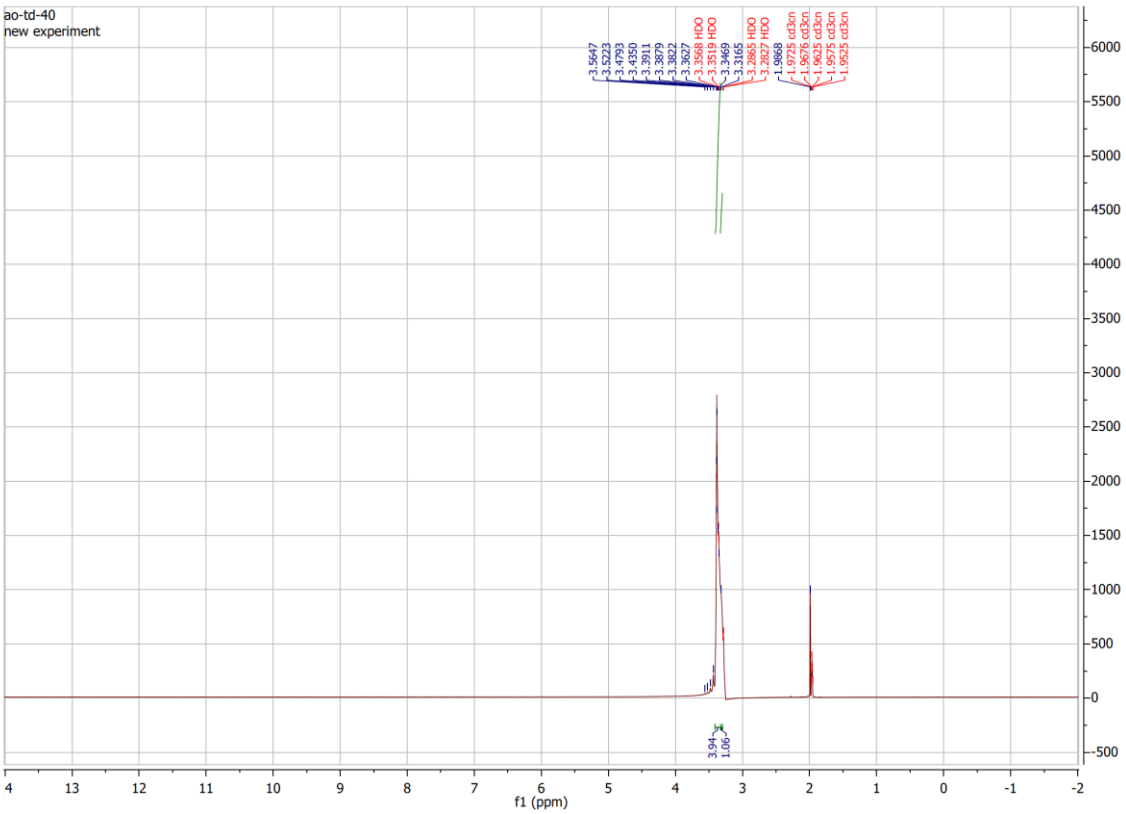

Figure SI-2: ^{1}H-NMR spectrum of LiTDI

4.1.2 LiPDI

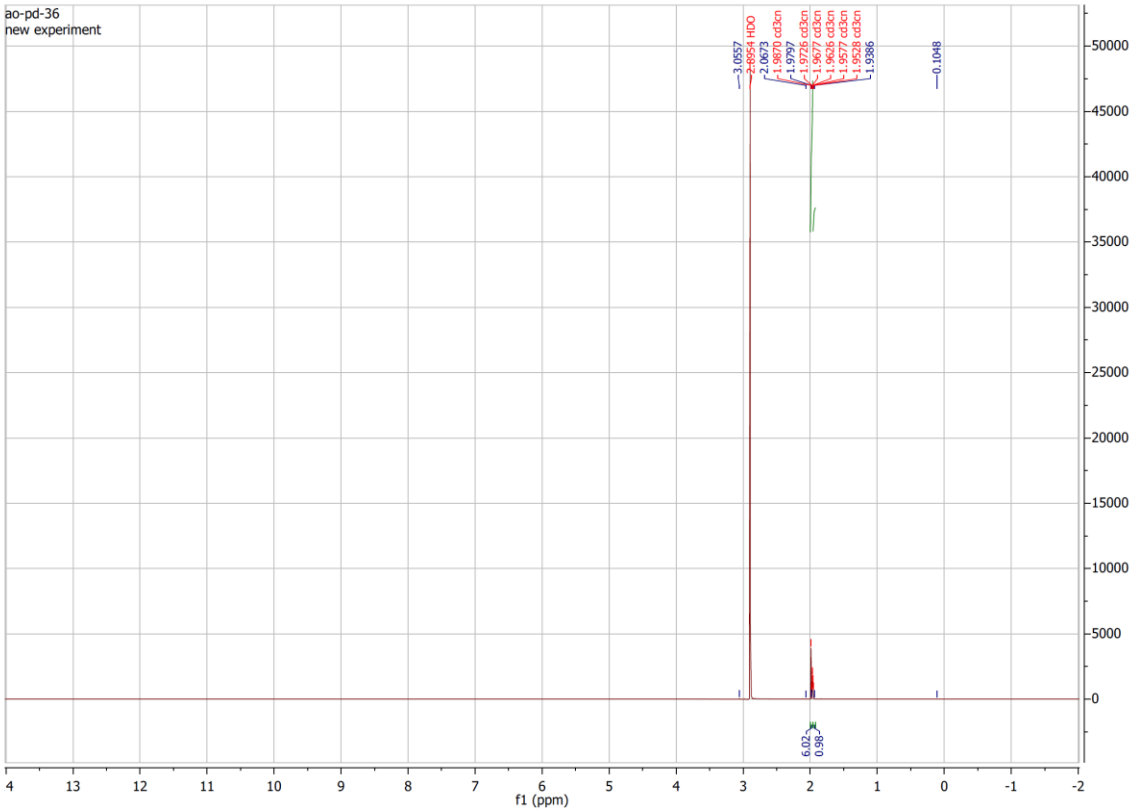

Figure SI-3: ^{1}H-NMR spectrum of LiPDI

4.1.3 LiHDI

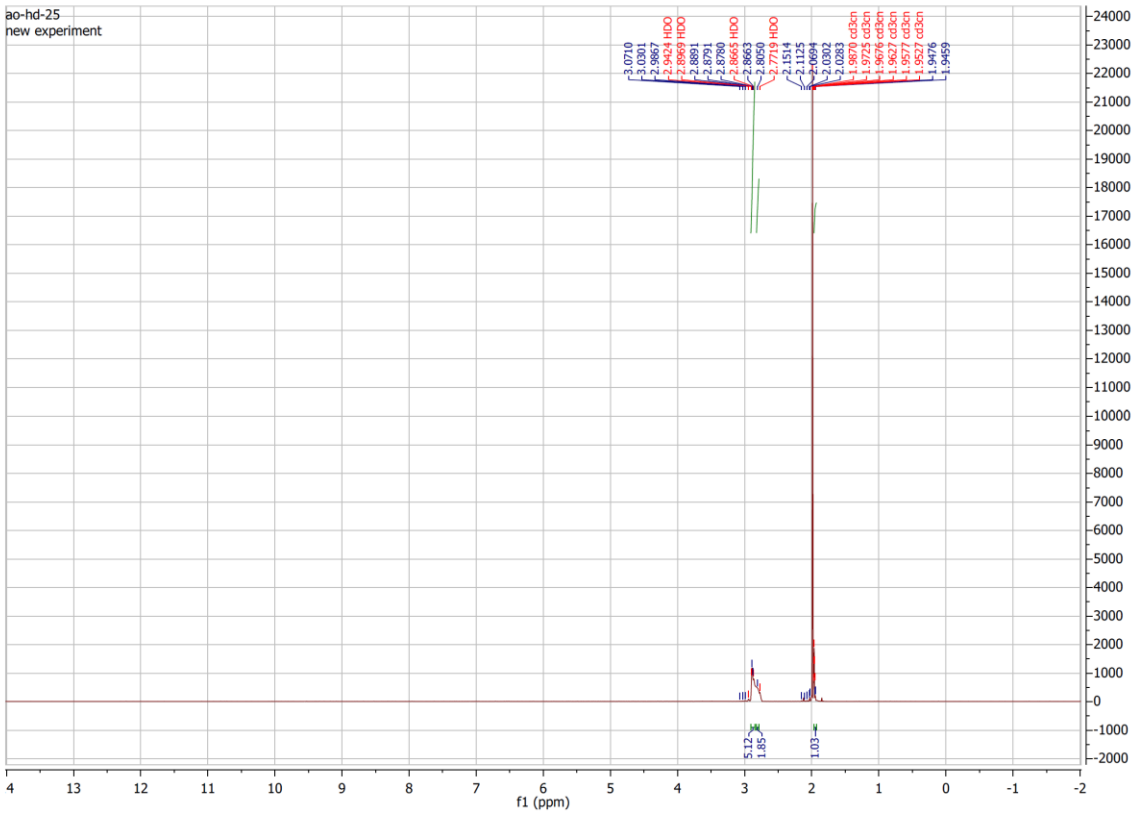

Figure SI-4: ^{1}H-NMR spectrum of LiHDI

4.2 ^{19}F-NMR

4.2.1 LiTDI

In the ^{19}F NMR spectrum for LiTDI shown in Figure SI-5, a diagnostic signal at δ = -64.24 ppm originating from the -CF_3 group was observed.

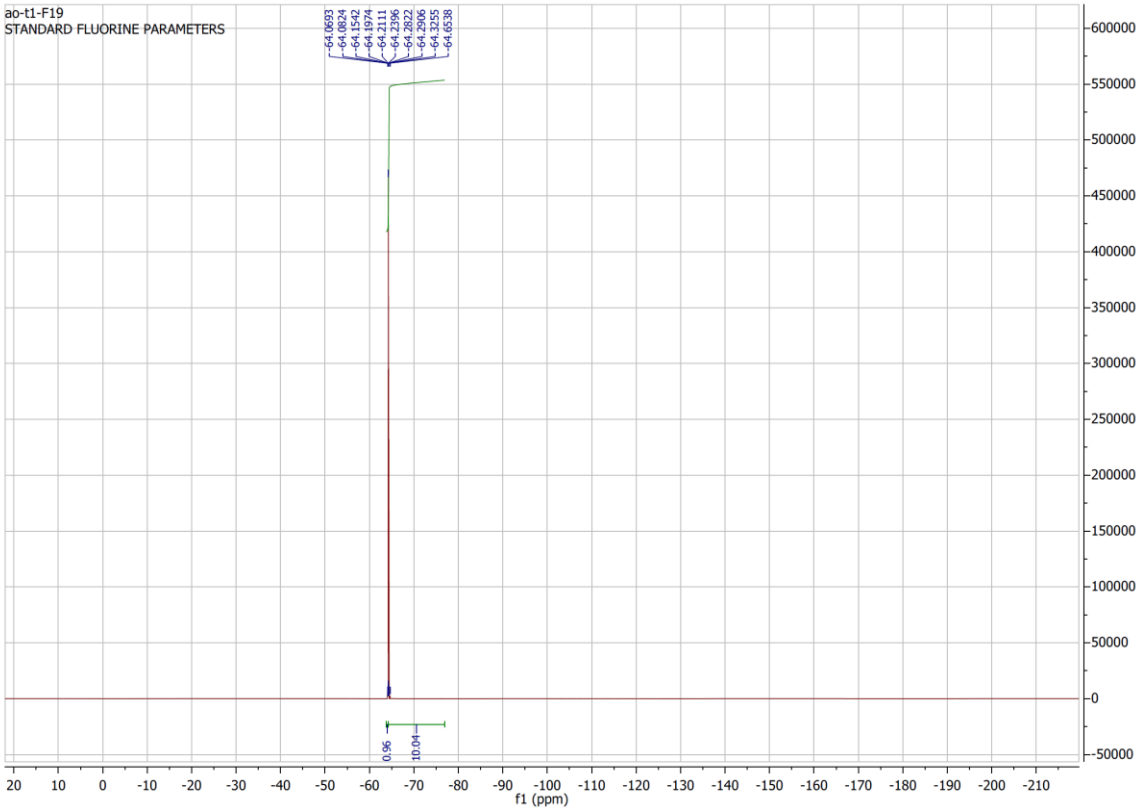

Figure SI-5: ^{19}F-NMR spectrum of LiTDI.

4.2.2 LiPDI

In the ^{19}F NMR spectrum for LiPDI presented in Figure SI-6, we observed two diagnostic signals at δ = -84.24 ppm originating from the $-CF_3$ group and at δ = -112.31 ppm corresponding to the $-CF_2$ group of the molecule.

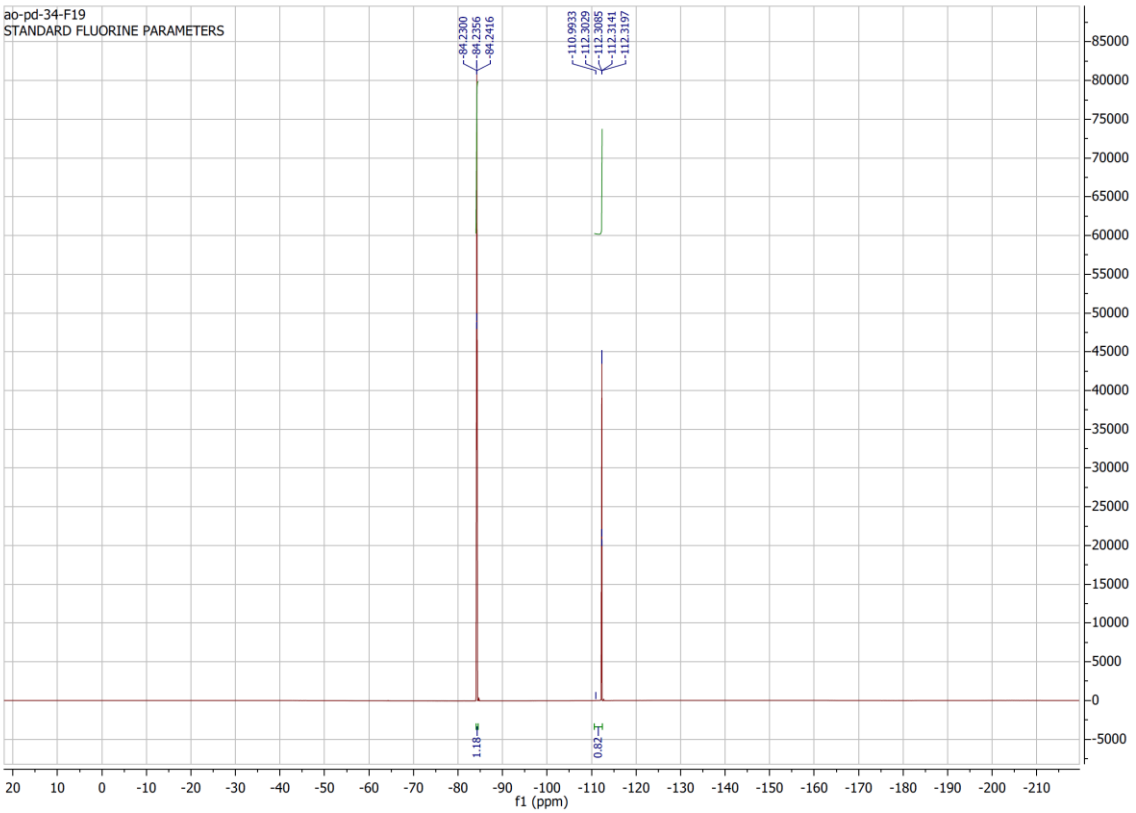

Figure SI-6: ^{19}F-NMR spectrum of LiPDI.

4.2.3 LiHDI

For LiHDI, we observed three diagnostic signals in the ^{19}F spectrum presented in Figure SI-7 at δ = -81.31 ppm originating from the -CF_3 group, δ = -111.22 ppm, and at δ = -127.39 ppm with the latter two corresponding to the -CF_2 groups present in the molecule.

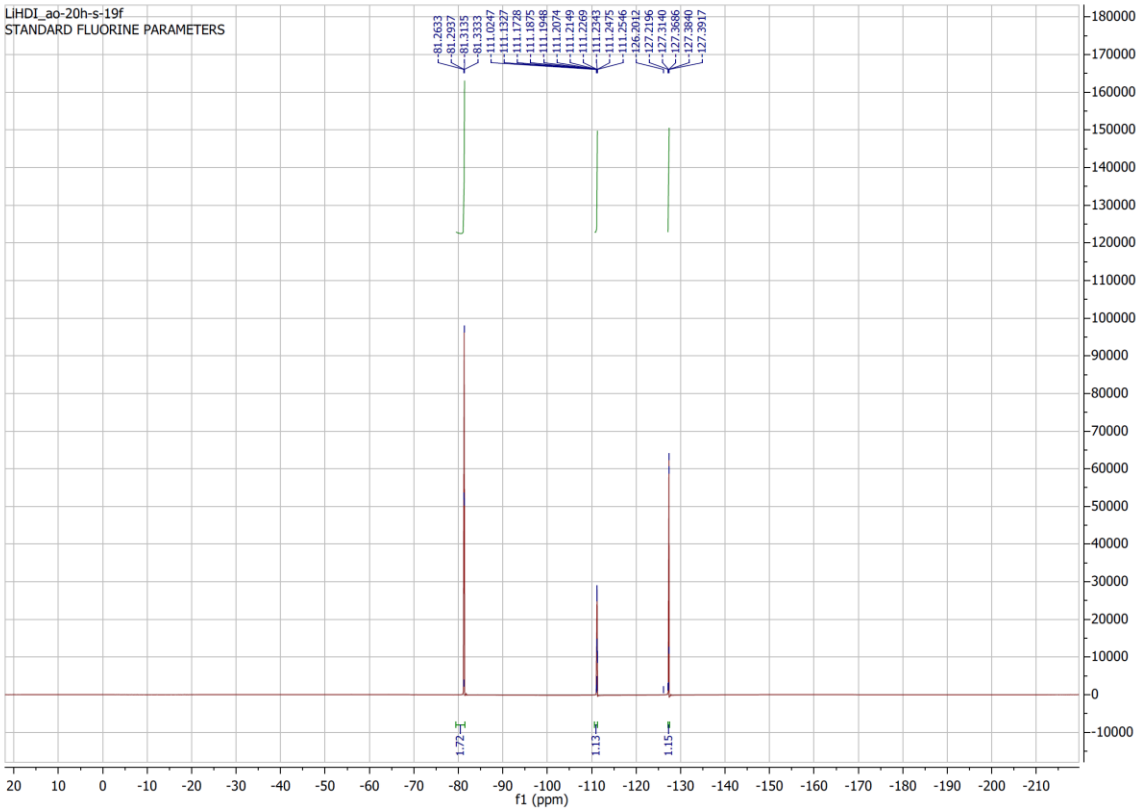

Figure SI-7: Total view of the ^{19}F-NMR spectrum of LiHDI.

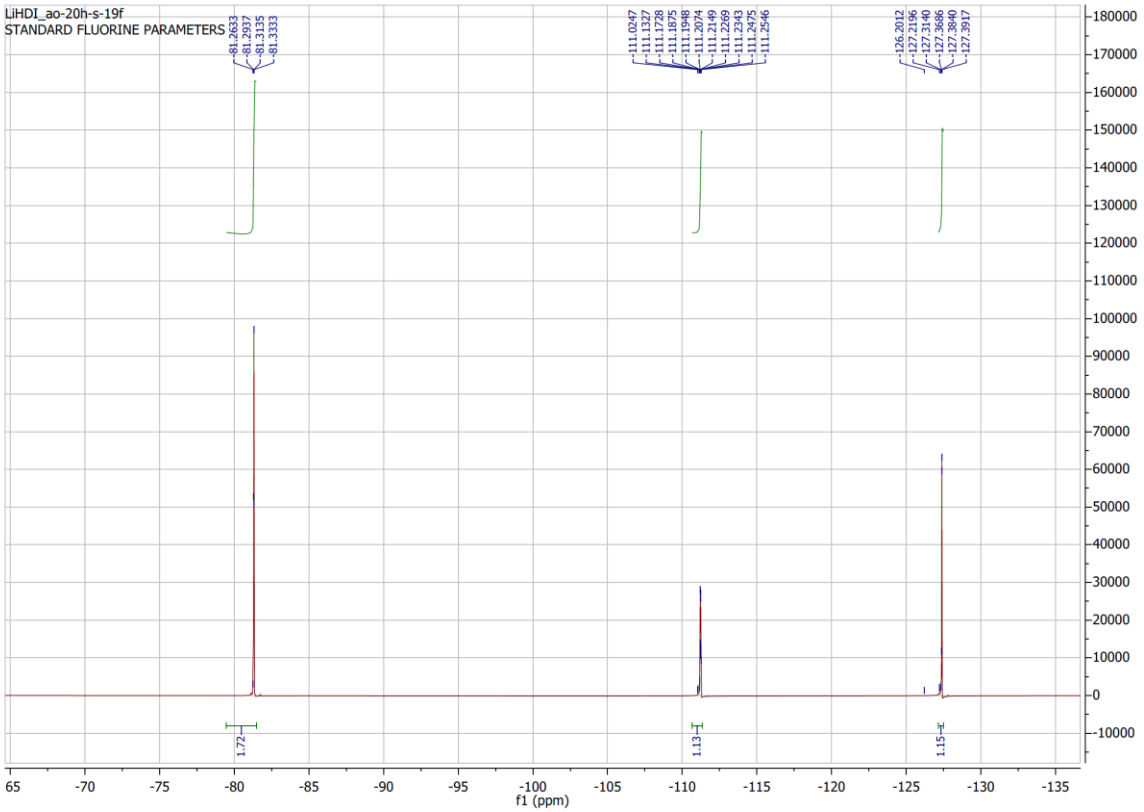

Figure SI-8: Enlarged view of the ^{19}F-NMR spectrum of LiHDI in the range from approx. -137 ppm to 65 ppm.

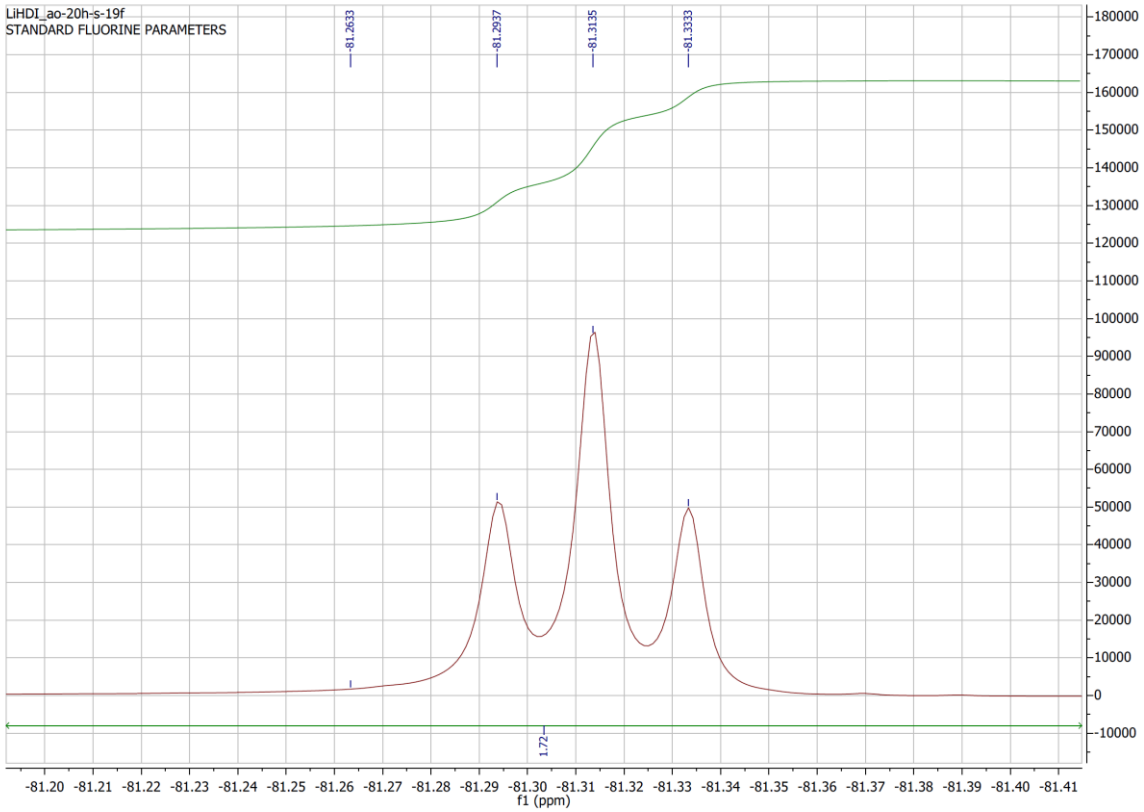

Figure SI-9: Enlarged view of the ^{19}F-NMR spectrum of LiHDI in the range from approx. -81.5 ppm to -81.2 ppm.

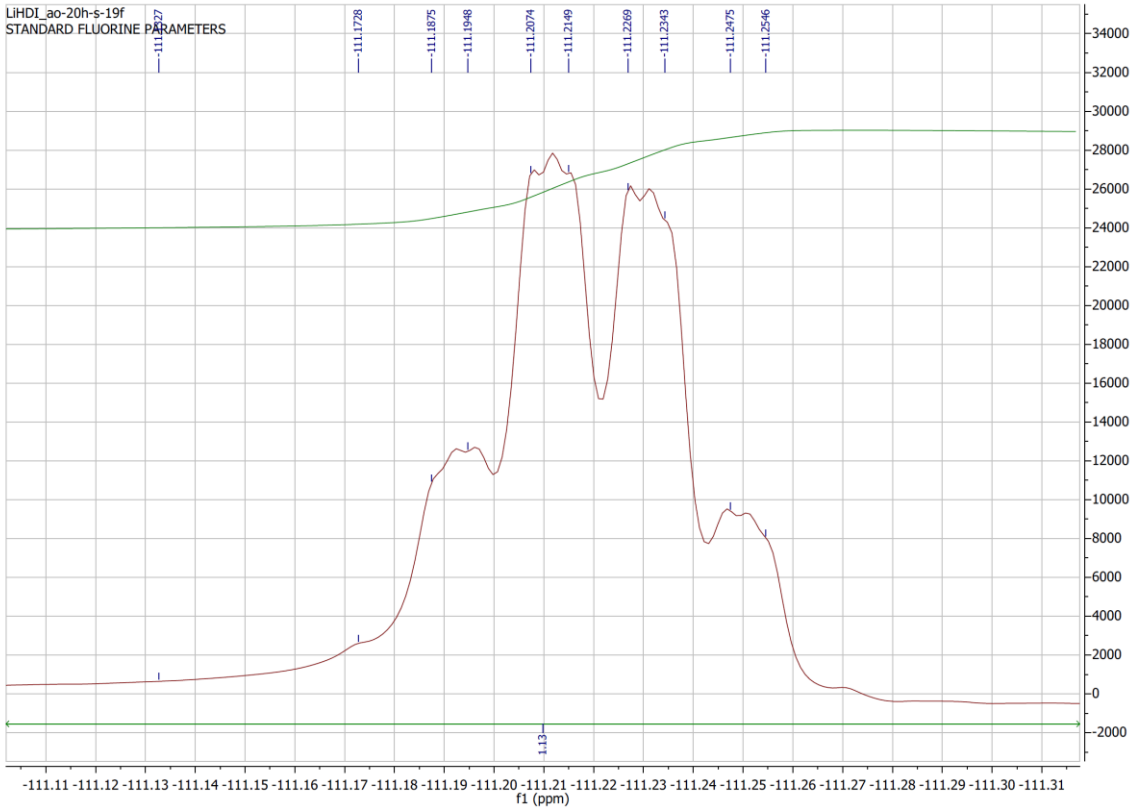

Figure SI-10: Enlarged view of the ^{19}F-NMR spectrum of LiHDI in the range from approx. -111.32 ppm to -111.10 ppm.

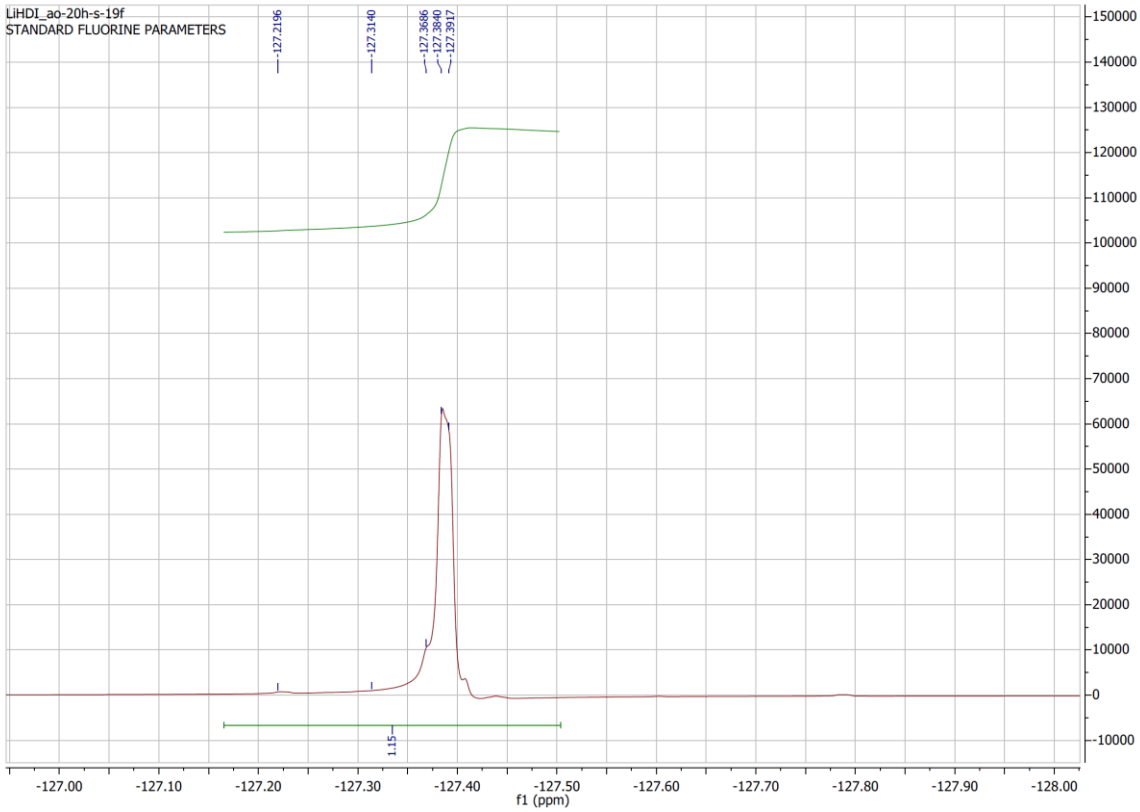

Figure SI-11: Enlarged view of the ^{19}F-NMR spectrum of LiHDI in the range from approx. -128.03 ppm to -126.95 ppm.

4.3 ^{13}C-NMR

All ^{13}C NMR spectra for LiTDI, LiPDI, and LiHDI were in agreement with those published in literature[2].

4.3.1 LiTDI

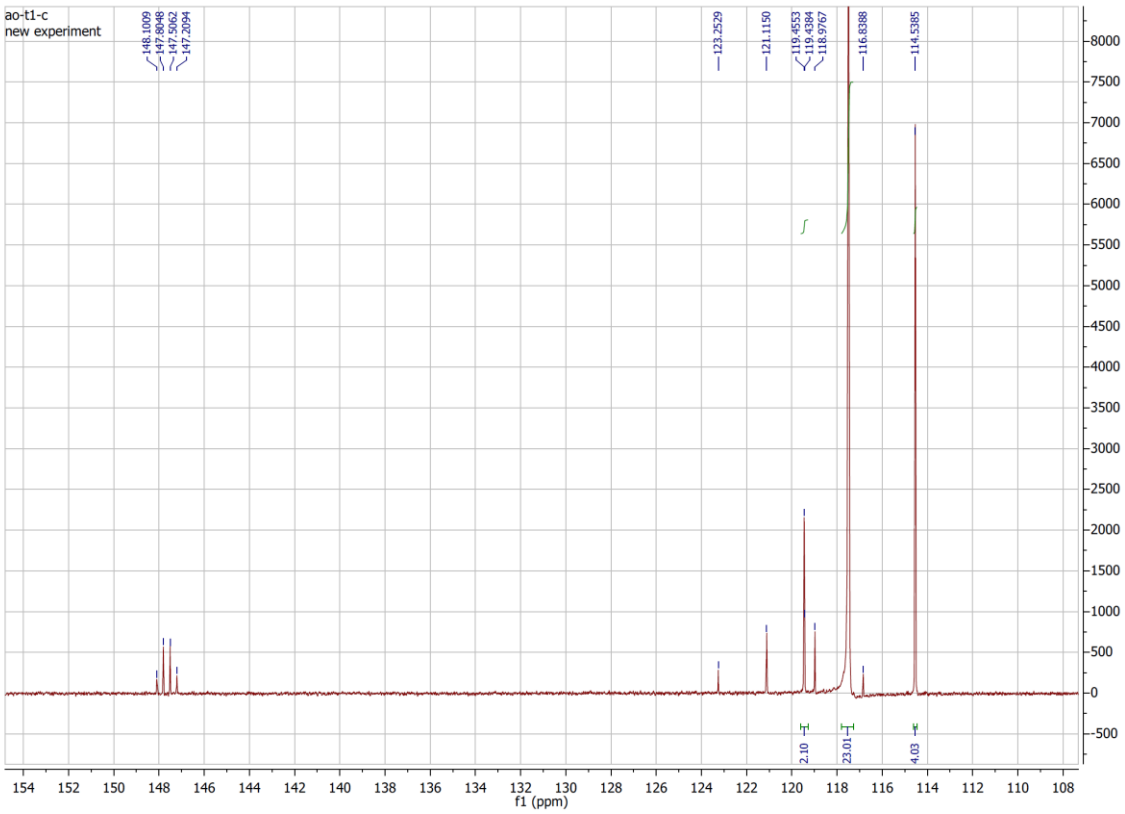

Figure SI-12: Total view of the ^{13}C-NMR spectrum of LiTDI.

4.3.2 LiPDI

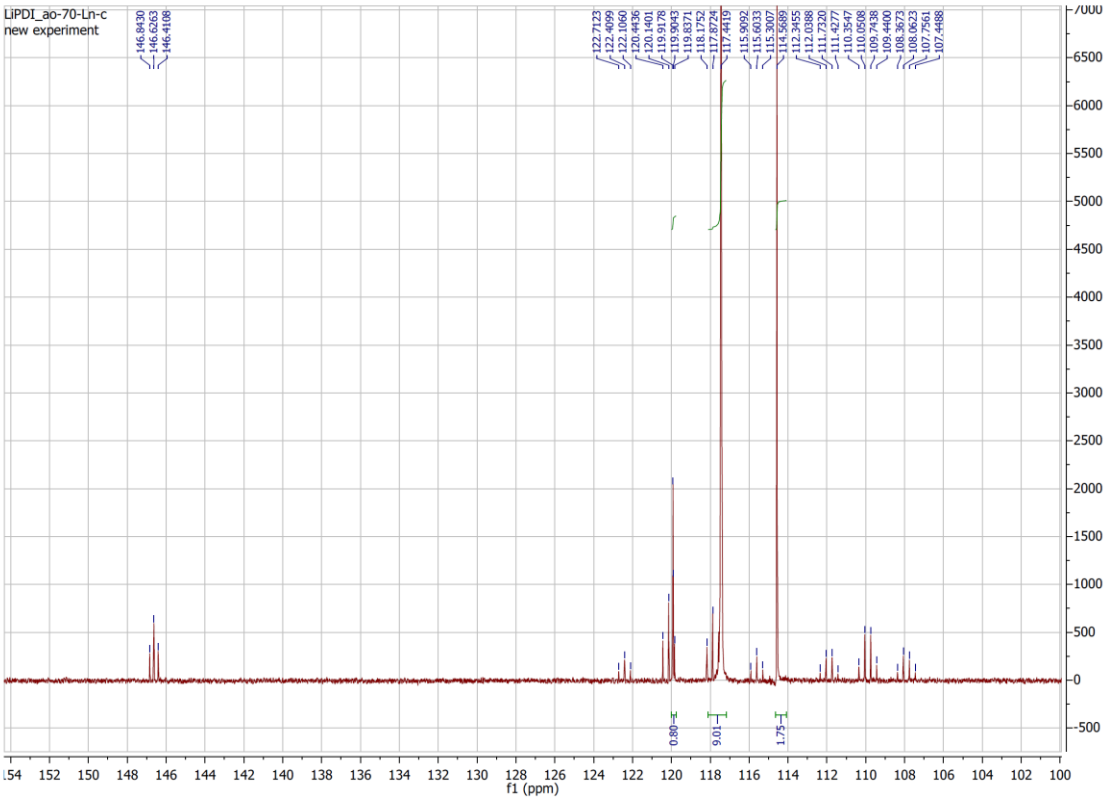

Figure SI-13: Total view of the ^{13}C-NMR spectrum of LiPDI.

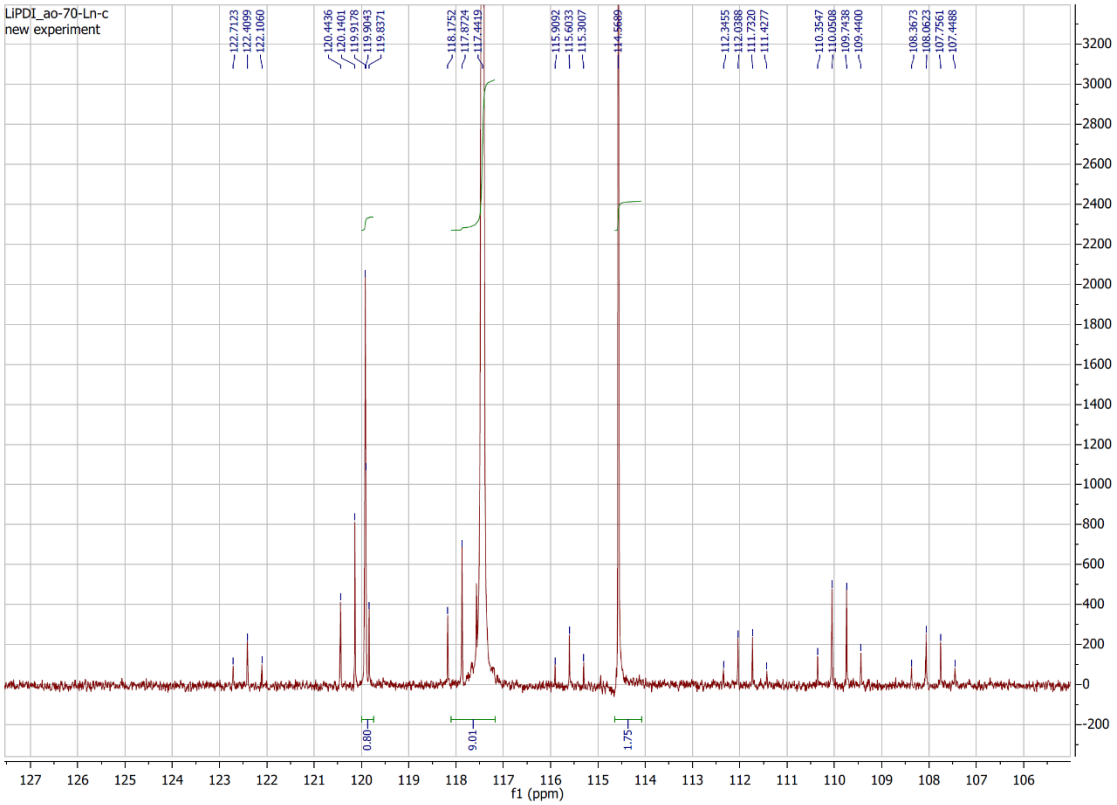

Figure SI-14: Enlarged view of the ^{13}C-NMR spectrum of LiPDI in the range between approx. 105 ppm and 127.5 ppm.

4.3.3 LiHDI

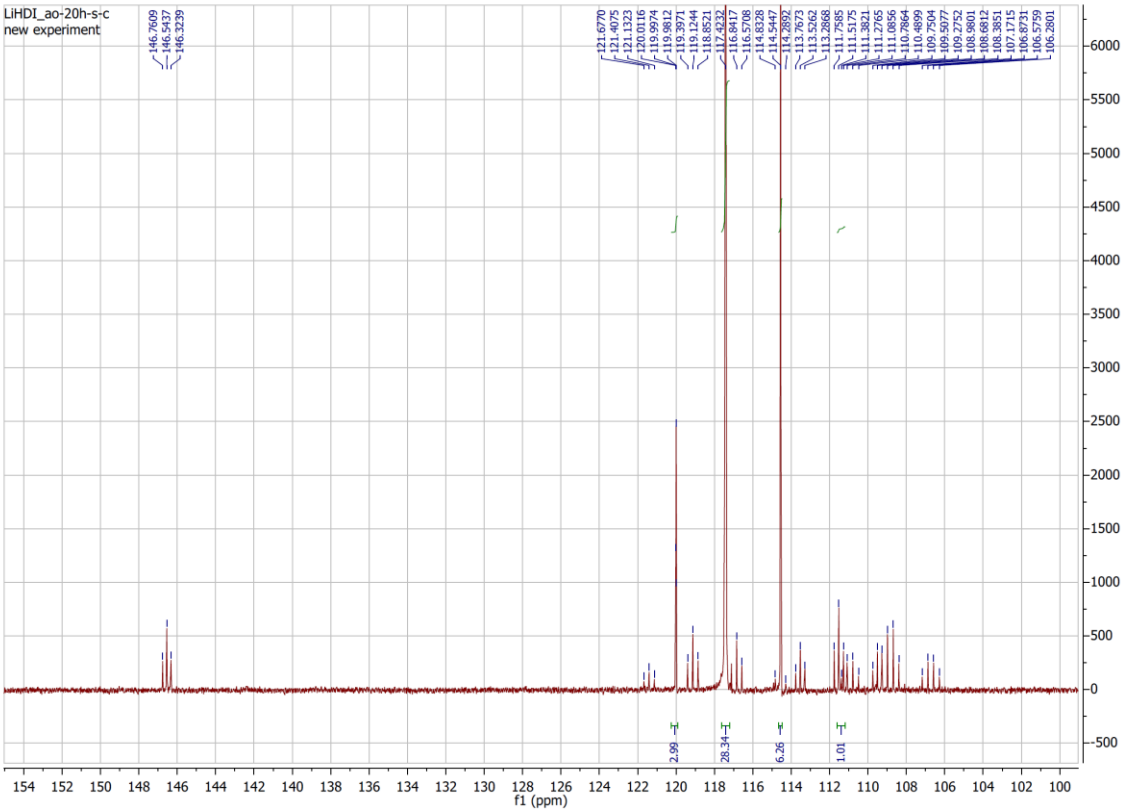

Figure SI-15: ^{13}C-NMR spectrum of LiHDI.

4.4 ^{7}Li-NMR

Some of the lithium spectra show signals additional to the main signal.

4.4.1 LiTDI

	Parameter	Value
1	Title	LiTDI_Li7
2	Origin	Varian
3	Spectrometer	vnmrs
4	Solvent	d2o
5	Temperature	25.0
6	Pulse Sequence	s2pul
7	Number of Scans	540
8	Acquisition Time	0.1990
9	Spectrometer Frequency	194.27
10	Nucleus	7Li

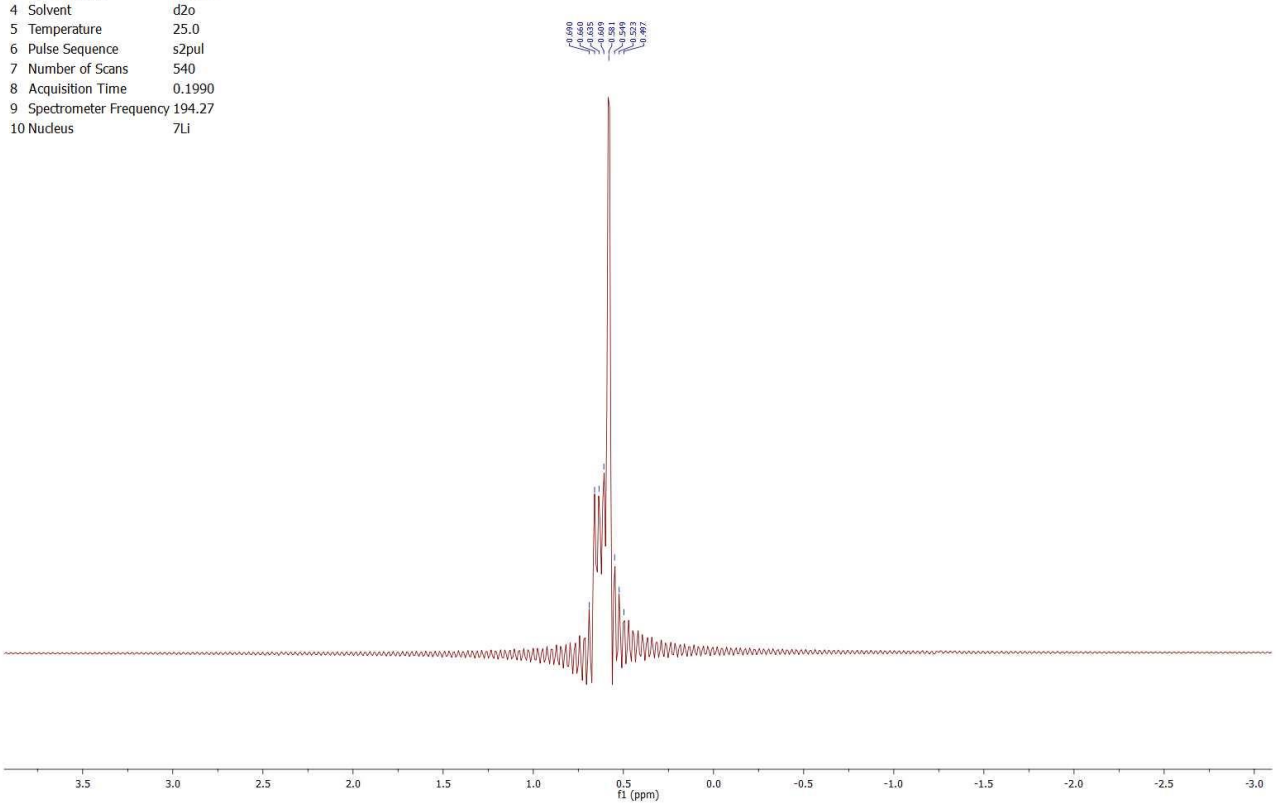

Figure SI-16a: ^{7}Li-NMR spectrum of LiTDI.

4.4.2 LiPDI

	Parameter	Value
1	Title	niebieski_Li7
2	Origin	Varian
3	Spectrometer	vnmrs
4	Solvent	d2o
5	Temperature	25.0
6	Pulse Sequence	s2pul
7	Number of Scans	680
8	Acquisition Time	0.1990
9	Spectrometer Frequency	194.27
10	Nucleus	7Li

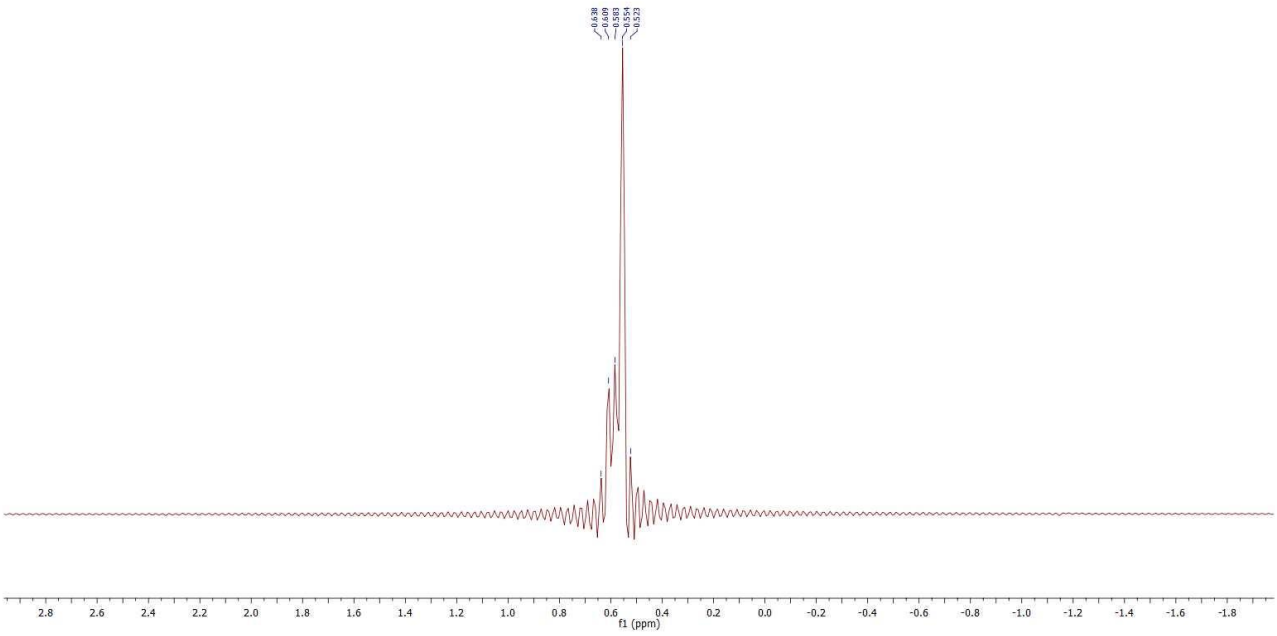

Figure SI-16b: ^{7}Li-NMR spectrum of LiPDI.

4.4.3 LiHDI

	Parameter	Value
1	Title	zolty_Li7
2	Origin	Varian
3	Spectrometer	vnmrs
4	Solvent	d2o
5	Temperature	25.0
6	Pulse Sequence	s2pul
7	Number of Scans	480
8	Acquisition Time	0.1990
9	Spectrometer Frequency	194.27
10	Nucleus	7Li

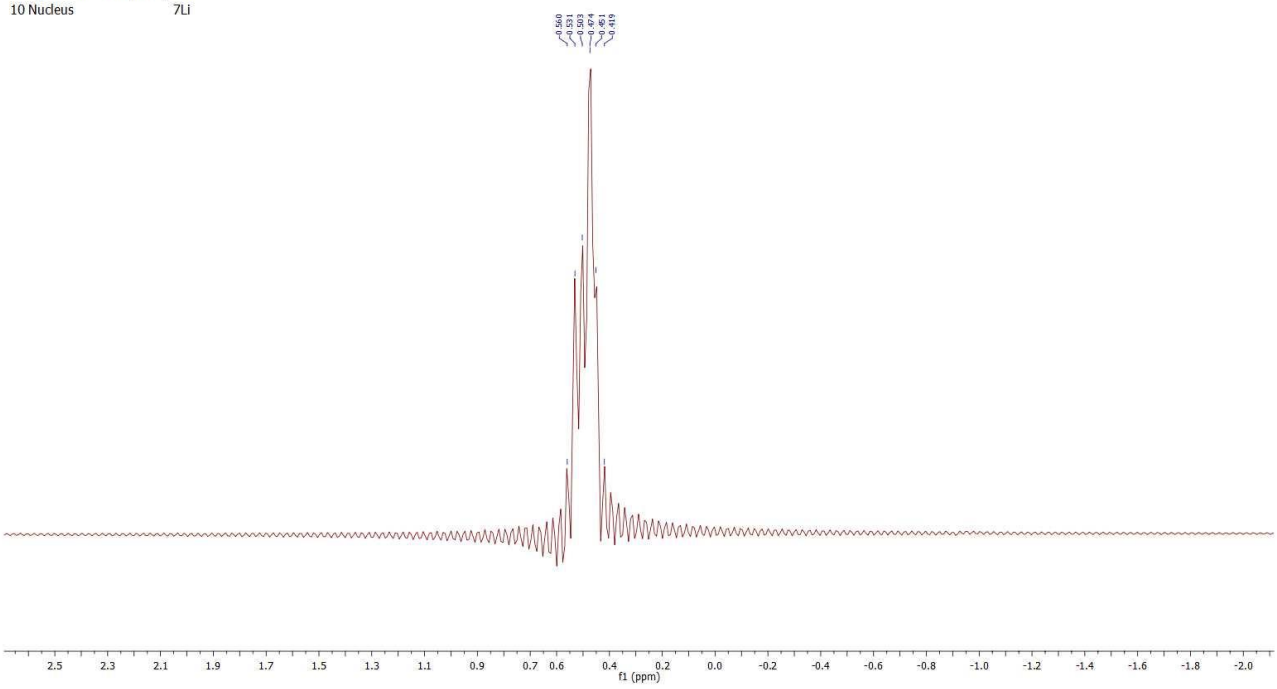

Figure SI-16c: ^{7}Li-NMR spectrum of LiHDI.

4.4.4 $LiPF_6$

	Parameter	Value
1	Title	niebieski_Li7
2	Origin	Varian
3	Spectrometer	vnmrs
4	Solvent	d2o
5	Temperature	25.0
6	Pulse Sequence	s2pul
7	Number of Scans	680
8	Acquisition Time	0.1990
9	Spectrometer Frequency	194.27
10	Nucleus	7Li

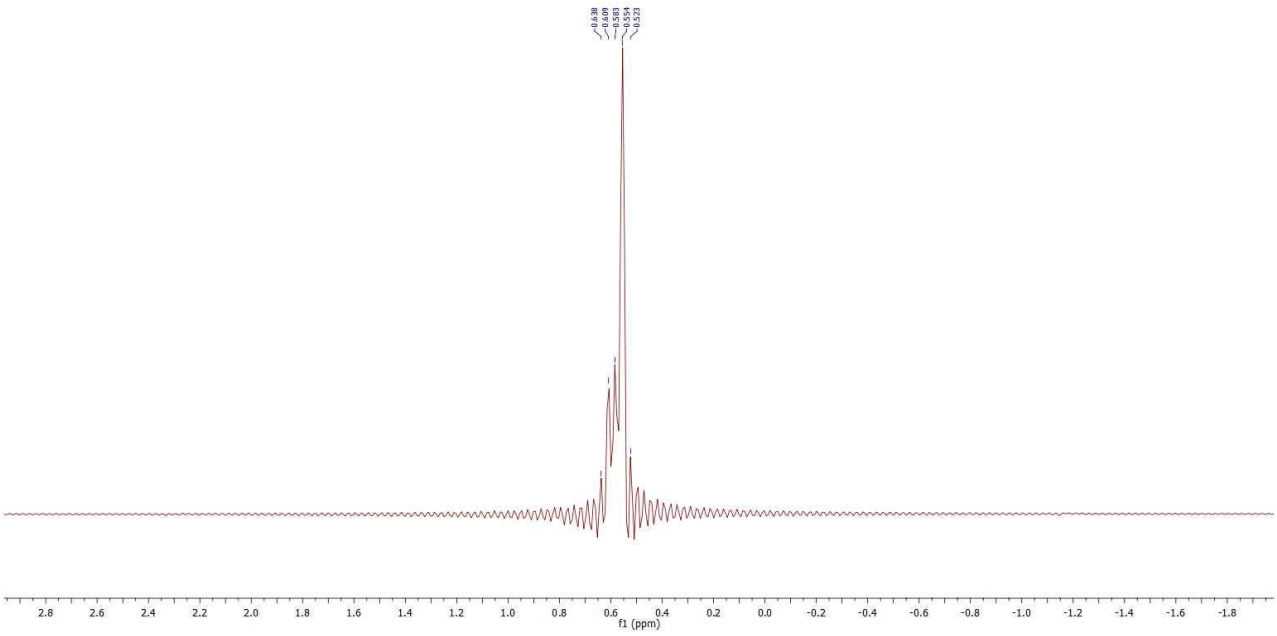

Figure SI-16d: ^{7}Li-NMR spectrum of $LiPF_6$.

5 FTIR and Raman spectra of the pure salts

For each salt three spectral ranges, the full spectrum and the ranges of ring vibrations (1550 cm^{-1} – 650 cm^{-1}) and vibrations of the CN nitrile groups were applied to present a deep analysis of LiPDI and LiHDI salts using Raman and FTIR methods. The CN stretching vibration band in spectra of the crystalline LiPDI and LiHDI solvates with 12C4 exhibits a split, with a separation between the bands equal to ~8 cm^{-1}. Such an effect was not found for the previously studied LiTDI solvates and may arise due to the longer alkylchain of the $-C_2F_5$ and $-C_3F_7$ substituents as compared with $-CF_3$ in the TDI^- anion. Increasing temperature results in merging of the bands in the spectra of the melted solvate, with the position of the resulting peak averaged between the positions of the peaks in the crystalline state, e.g. 2225 cm^{-1} for LiHDI-12C4 melt as compared with 2227 cm^{-1} and 2218 cm^{-1} in the crystal. Bands originating from ring stretching and bending vibrations were not split and their position was almost the same before and after melting.

The analysis of the spectra of 15C5 complexes revealed significant difference between LiPDI and LiHDI. The spectral characteristic of the LiPDI-15C5 complex, with the position of the γCN band significantly shifted as compared with LiPDI-12C4, 2242 cm^{-1} and 2233 cm^{-1} vs 2227 cm^{-1} and 2219 cm^{-1}, but similar for the ring bending and stretching vibrations, points on the formation of the complex making use of the nitrile group. After melting, the positions of the anion bands is characteristic for the non-coordinated anion.

In spectra of LiHDI-15C5, bands characteristic for ring stretching and bending vibrations are either split, as in the case of δNCN vibration, or exhibit asymmetry, while the maximum of γCN band is shifted compared with molten LiHDI-12C4 (2230 cm^{-1} vs 2225 cm^{-1}), but the band is only slightly asymmetric. Such spectral features are characteristic for ionic pairs formed with use of the imidazolium nitrogen. After melting, the positions of the bands shift to values characteristic for ionic pairs, but the formation of a shoulder ~2240 cm^{-1}, clearly visible in Raman spectrum, is an evidence of partial aggregation of the salt.

5.1 LiPDI

5.1.1 In 12C4 crown ether

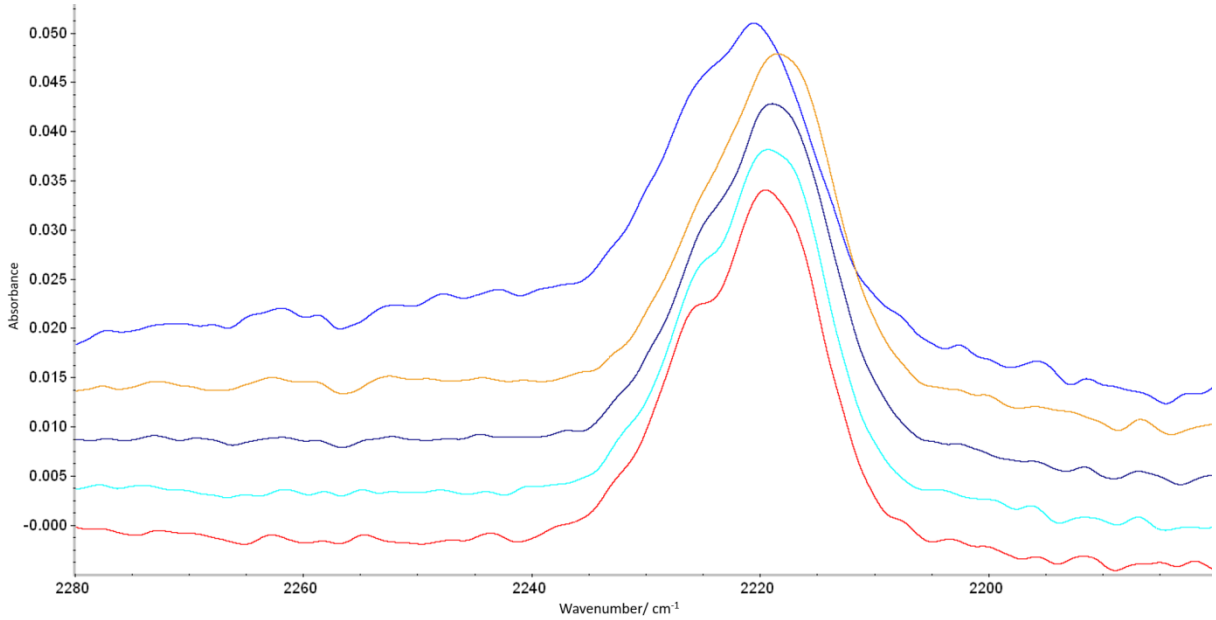

Figure SI-17: CN stretching vibration range in FTIR spectra of LiPDI-12C4 solvate in different temperatures: red - 30 °C, light blue - 50 °C, purple - 70 °C, yellow - 90 °C and blue - 120 °C.

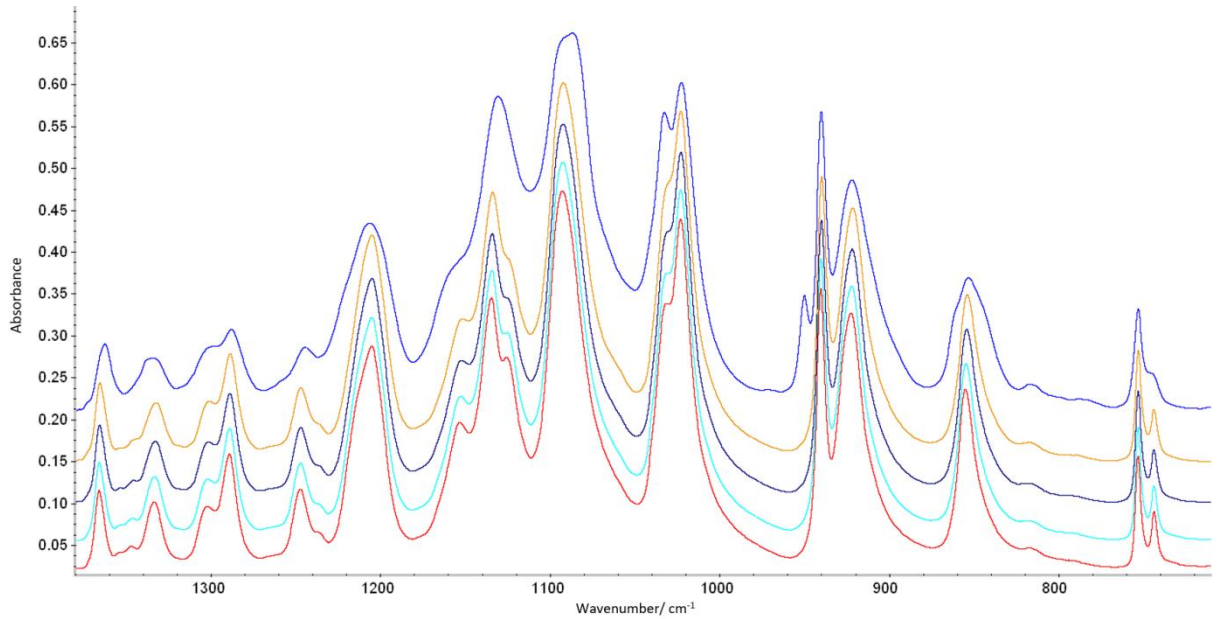

Figure SI-18: Imidazole ring bending (~940 cm^{-1}), C-O stretching and CH_2 rocking (900 cm^{-1} - 800 cm^{-1}) vibration range in FTIR spectra of LiPDI-12C4 solvate in different temperatures: red - 30 °C, light blue - 50 °C, purple - 70 °C, yellow - 90 °C and blue - 120 °C.

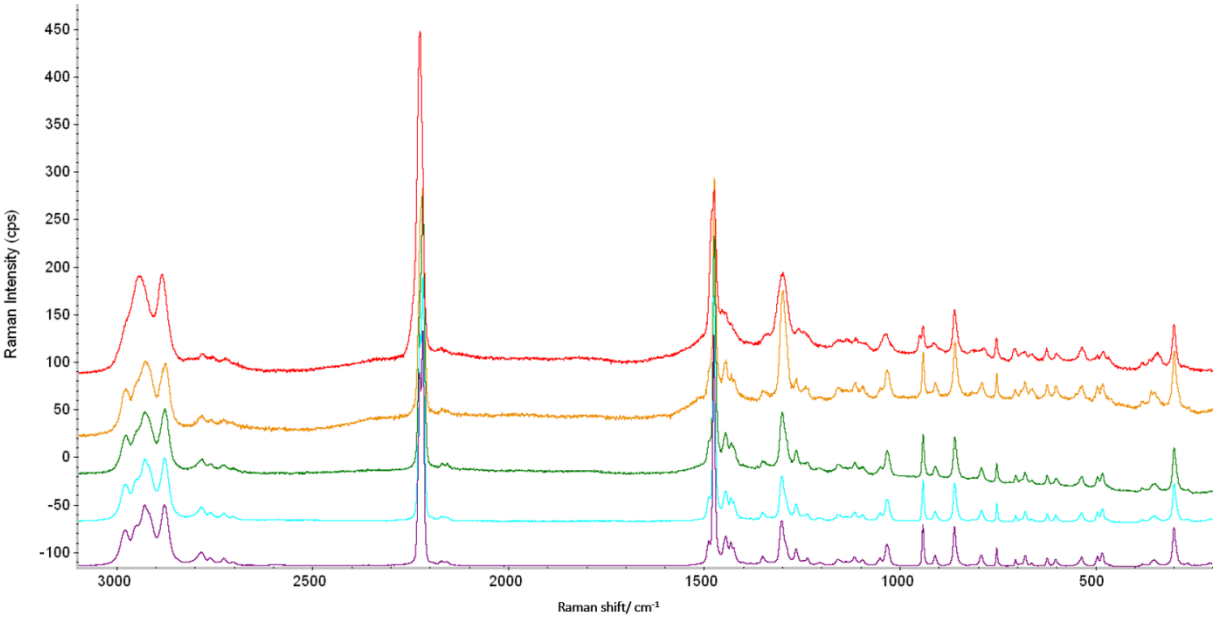

Figure SI-19: Raman spectra of LiPDI-12C4 solvate in different temperatures: purple - 30 °C, light blue - 50 °C, green - 60 °C (solution), orange - 90 °C (melted), red - 100 °C (aggregation).

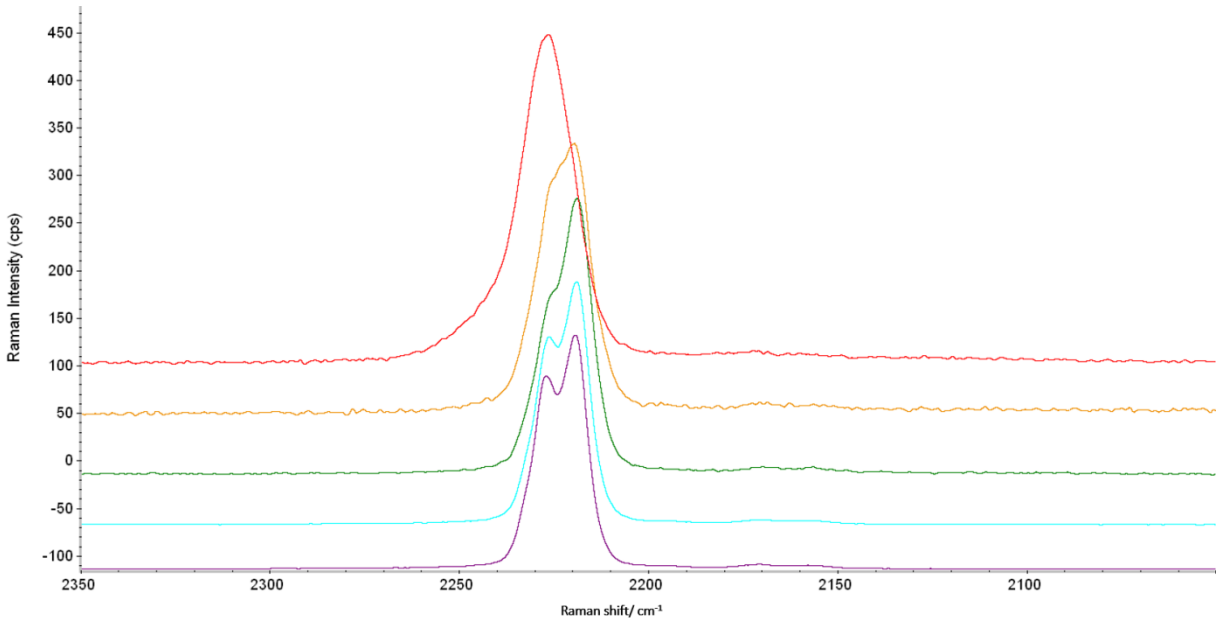

Figure SI-20: CN stretching vibration range in Raman spectrum of LiPDI-12C4 solvate in different temperatures: purple - 30 °C, light blue - 50 °C, green - 60 °C (solution), orange - 90 °C (melted), red - 100 °C (aggregation).

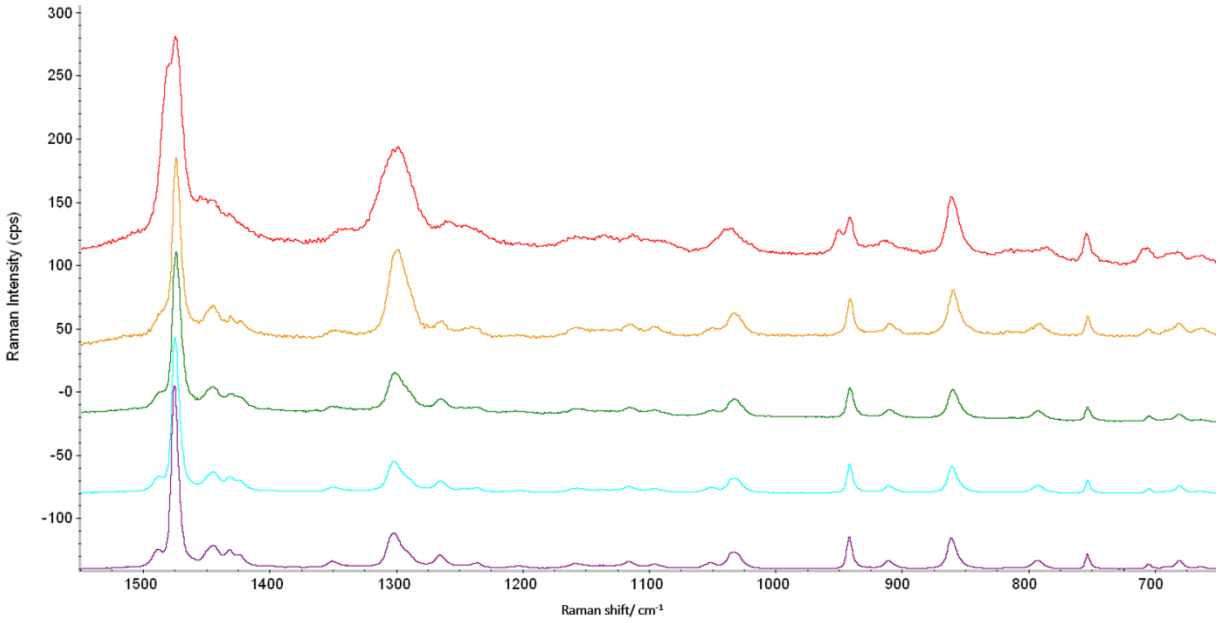

Figure SI-21: Imidazole ring stretching (1500 cm^{-1} - 1200 cm^{-1}), ring bending (~943 cm^{-1}) and CH_2 rocking (900 cm^{-1} - 800 cm^{-1}) vibration range in Raman spectra of LiPDI-12C4 in different temperatures: purple - 30 °C, light blue - 50 °C, green - 60 °C (solution), orange - 80 °C (melted), red - 100 °C (aggregation).

5.1.2 In 15C5 crown ether

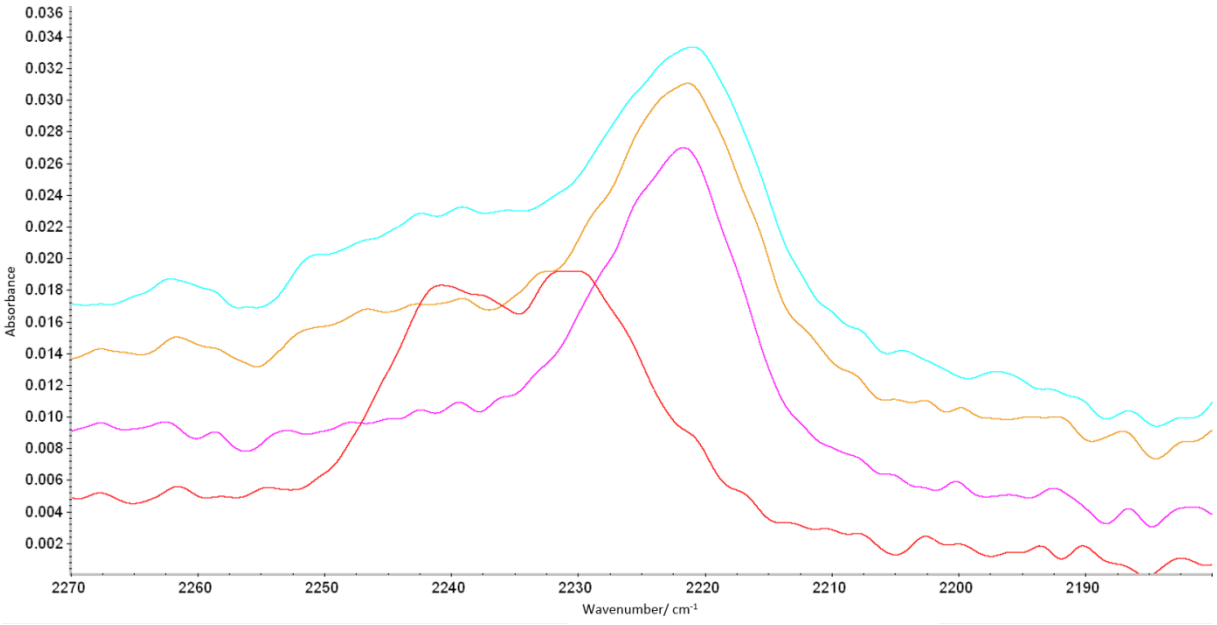

Figure SI-22: CN stretching vibration range in FTIR spectra of LiPDI-15C5 in different temperatures: red - 30 °C, pink - 40 °C, orange - 50 °C, and light blue - 60 °C (melted).

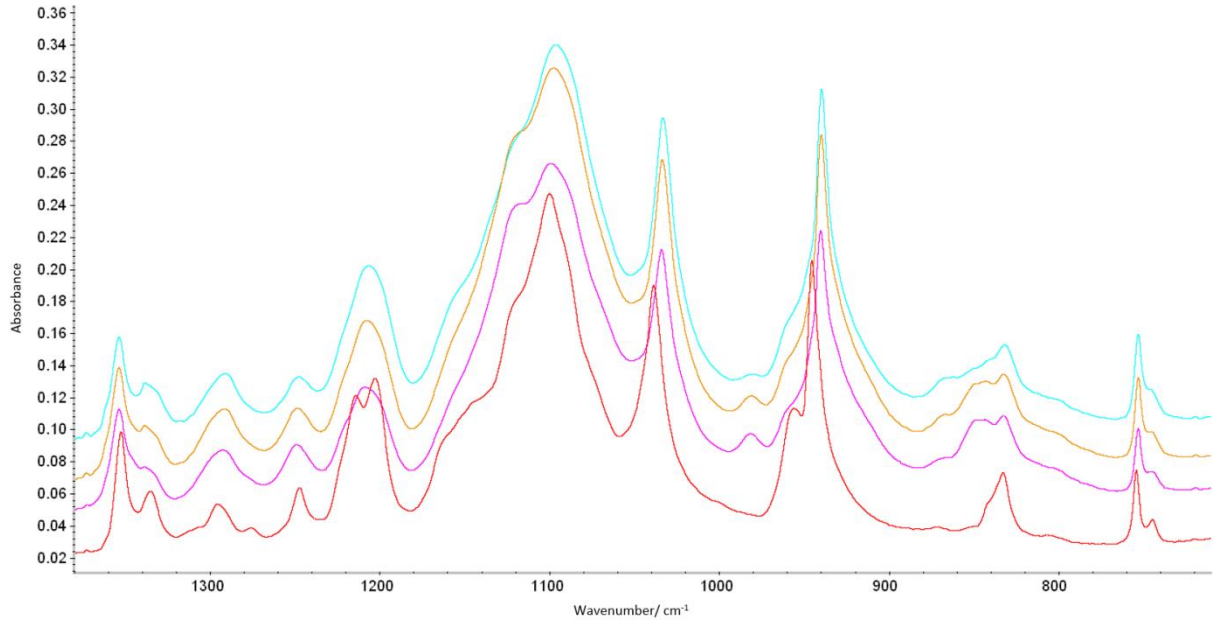

Figure SI-23: Imidazole ring bending (~940 cm^{-1}), C-O stretching and CH_2 rocking (900 cm^{-1} - 800 cm^{-1}) vibration range in FTIR spectra of LiPDI-15C5 solvate in different temperatures: red - 30 °C, pink - 40 °C, orange - 50 °C, and light blue - 60 °C (melted).

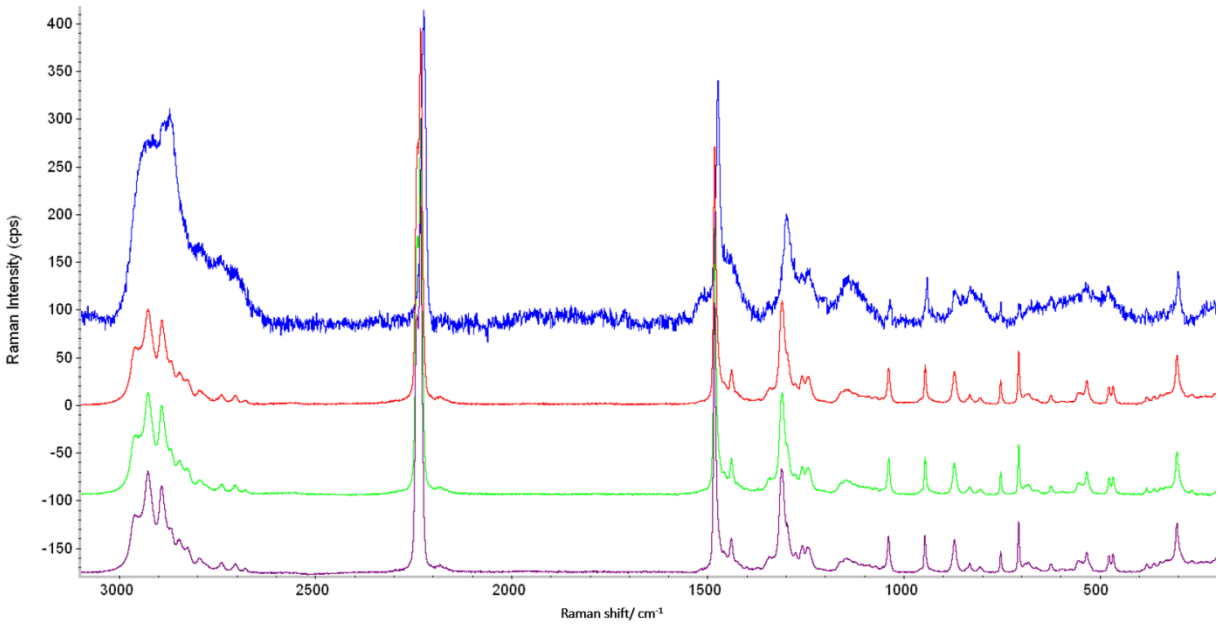

Figure SI-24: Raman spectra of LiPDI-15C5 in different temperatures: purple - 30 °C, green - 40 °C, red - 50 °C and blue - 60 °C (melted).

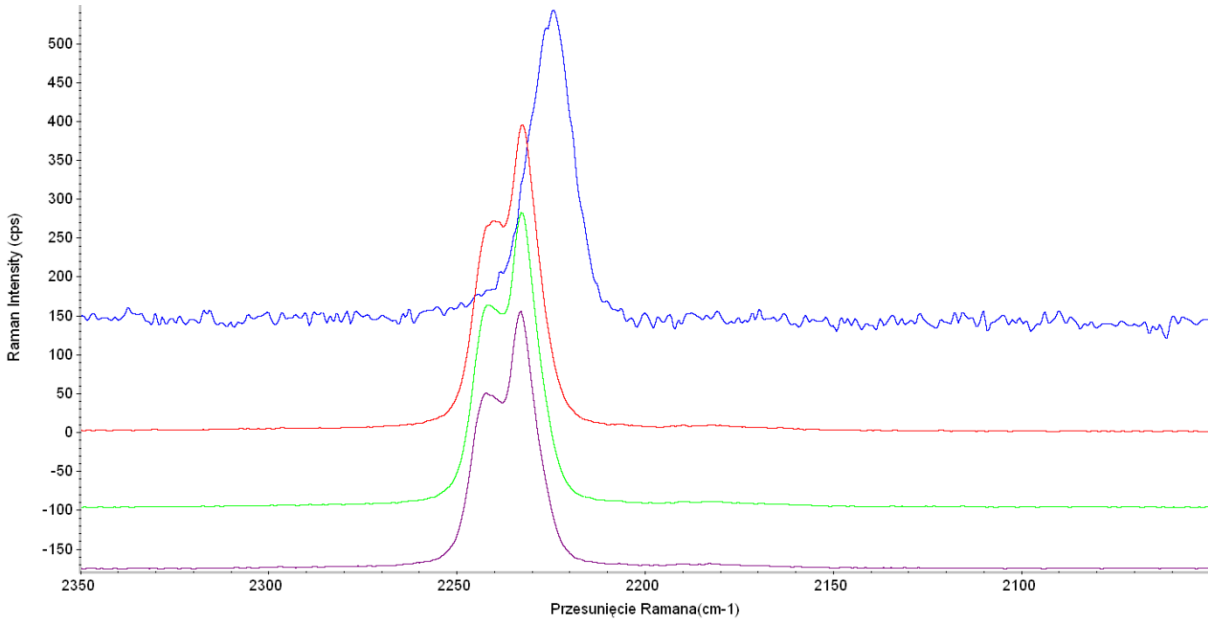

Figure SI-25: CN stretching vibration range in Raman spectra of LiPDI-15C5 in different temperatures: purple - 30 °C, green - 40 °C, red - 50 °C and blue - 60 °C (melted).

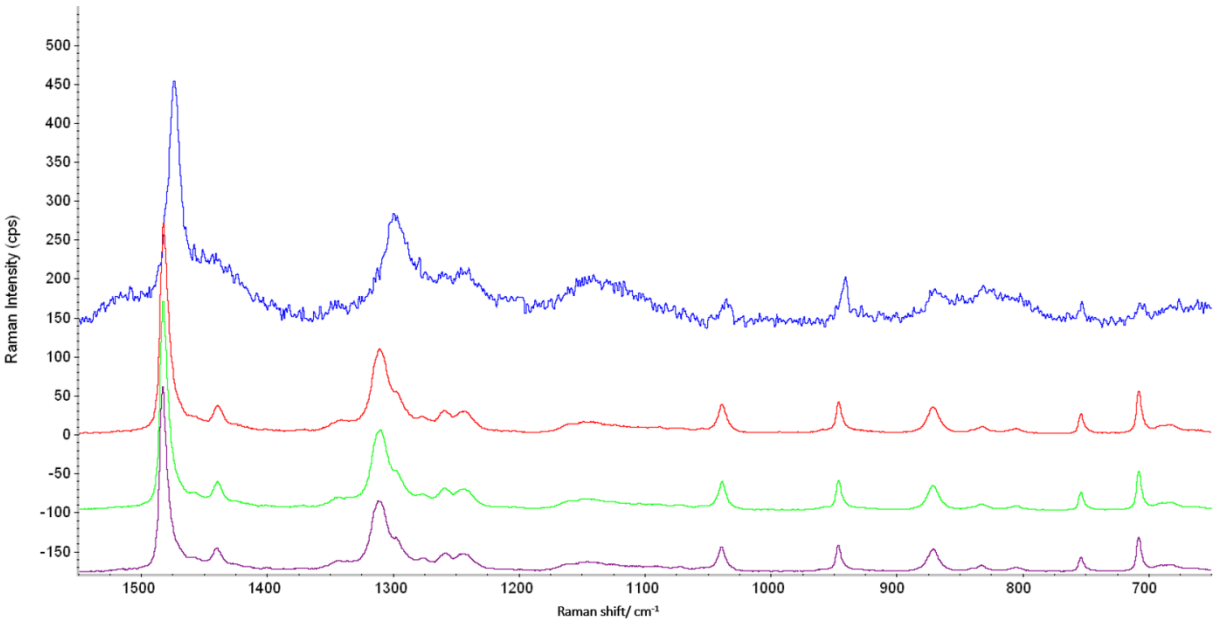

Figure SI-26: Imidazole ring stretching (1500 cm^{-1} - 1200 cm^{-1}), ring bending (~948 cm^{-1}) and CH_2 rocking (900 cm^{-1} – 800 cm^{-1}) vibration range in Raman spectra of LiPDI-15C5 in different temperatures: purple - 30 °C, green - 40 °C, red - 50 °C and blue - 60 °C (melted).

5.2 LiHDI

5.2.1 In 12C4 crown ether

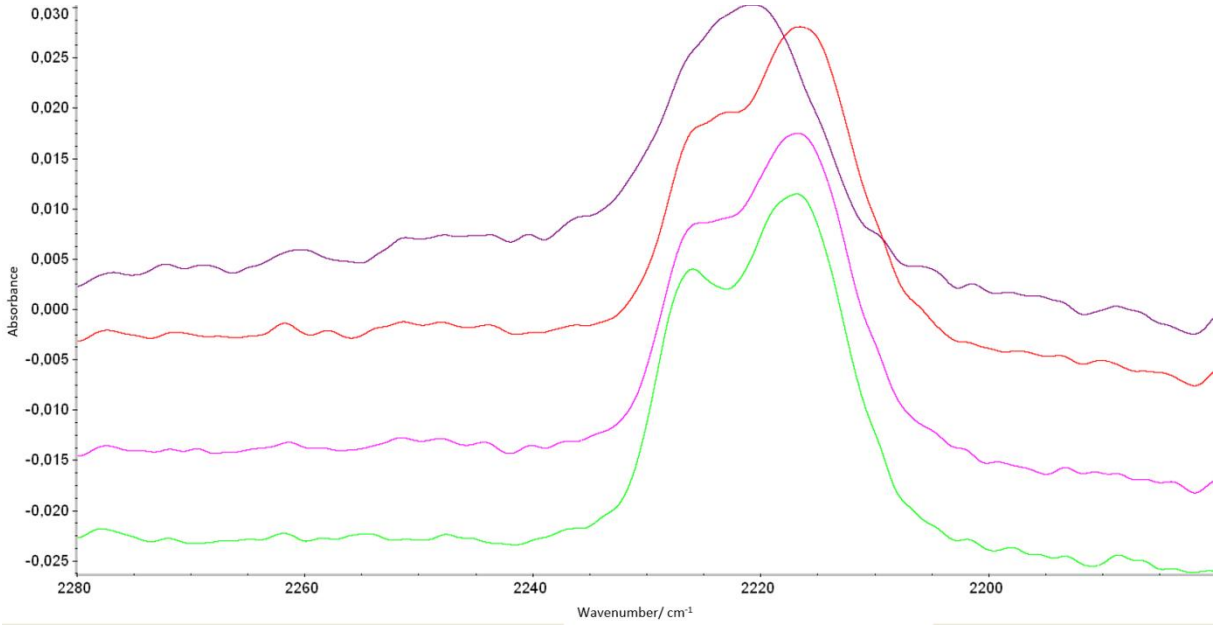

Figure SI-27: CN stretching vibration range in FTIR spectra of LiHDI-12C4 solvate in different temperatures: green - 40 °C, pink - 60 °C, red - 90 °C , and purple - 120 °C.

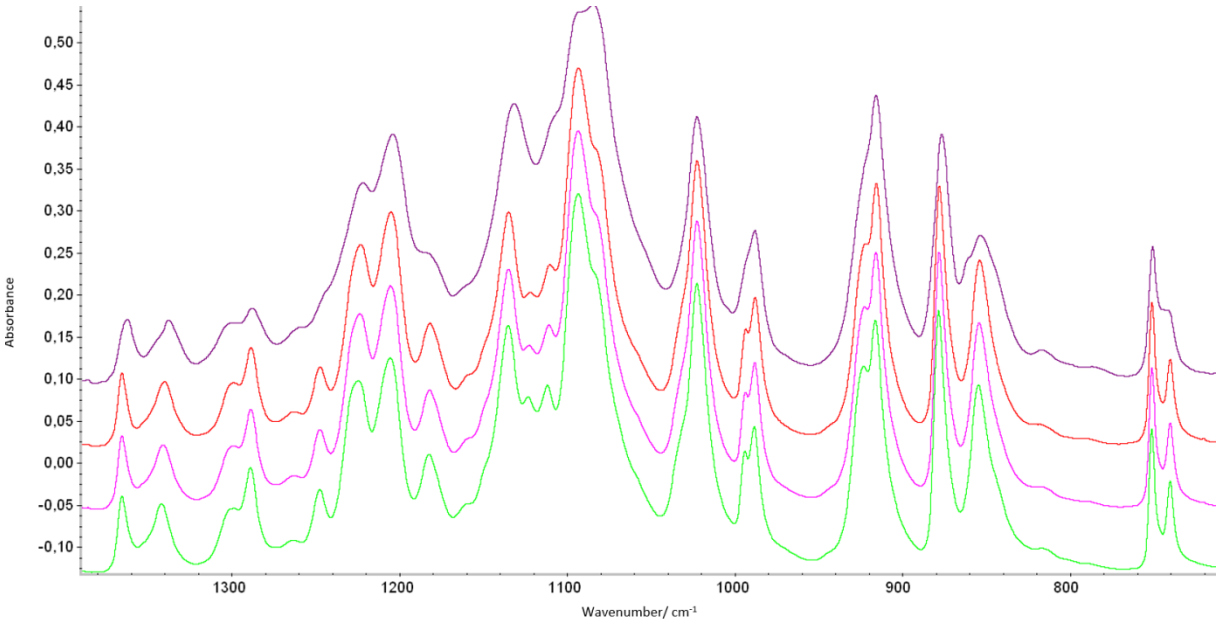

Figure SI-28: Imidazole ring bending (~990 cm^{-1}), C-O stretching and CH_2 rocking (900 cm^{-1} - 800 cm^{-1}) vibration range in FTIR spectra of LiHDI-12C4 in different temperatures: green - 40 °C, pink - 60 °C, red - 90 °C , and purple - 120 °C.

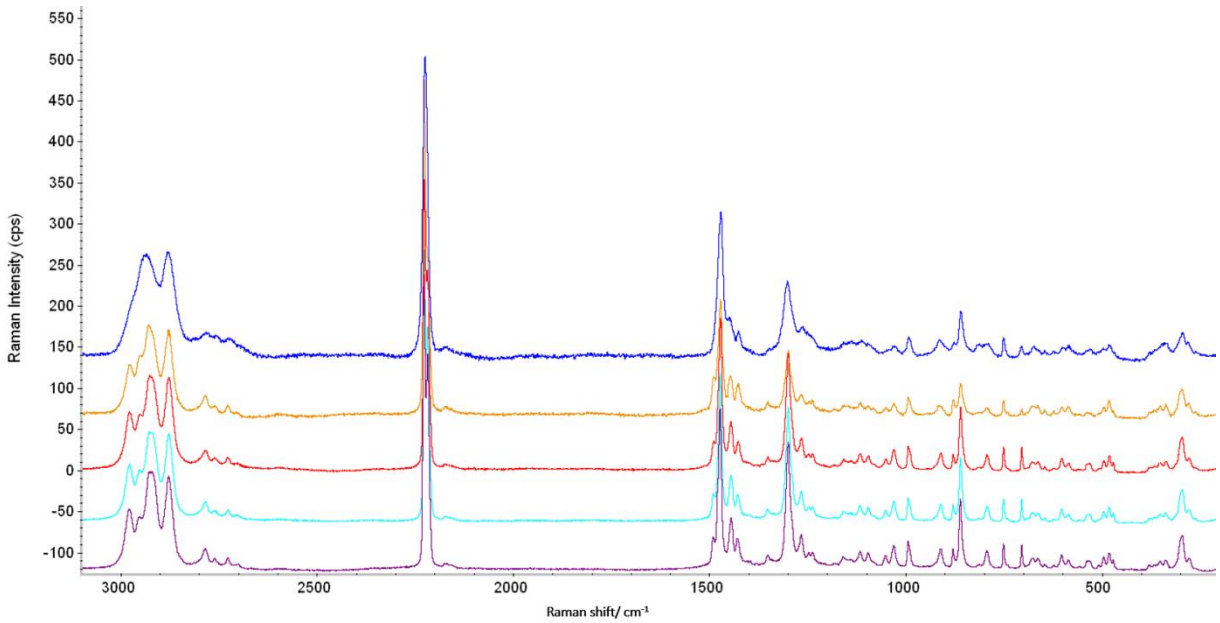

Figure SI-29: Raman spectra of LiHDI-12C4 solvate in different temperatures: purple - 30 °C, light blue - 50 °C, red - 70 °C, orange - 90 °C (melting started), and blue - 120 °C (melted).

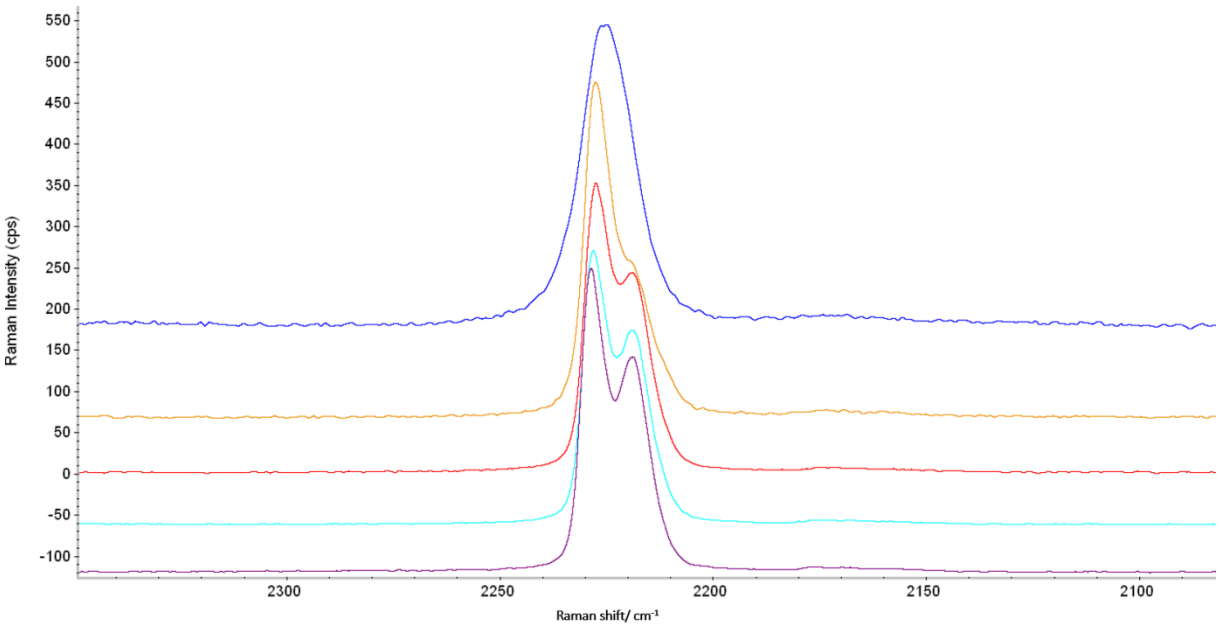

Figure SI-30: CN stretching vibration range in Raman spectra of LiHDI-12C4 solvate in different temperatures: purple - 30 °C, light blue - 50 °C, red - 70 °C, orange - 90 °C (melting started), and blue - 120 °C (melted).

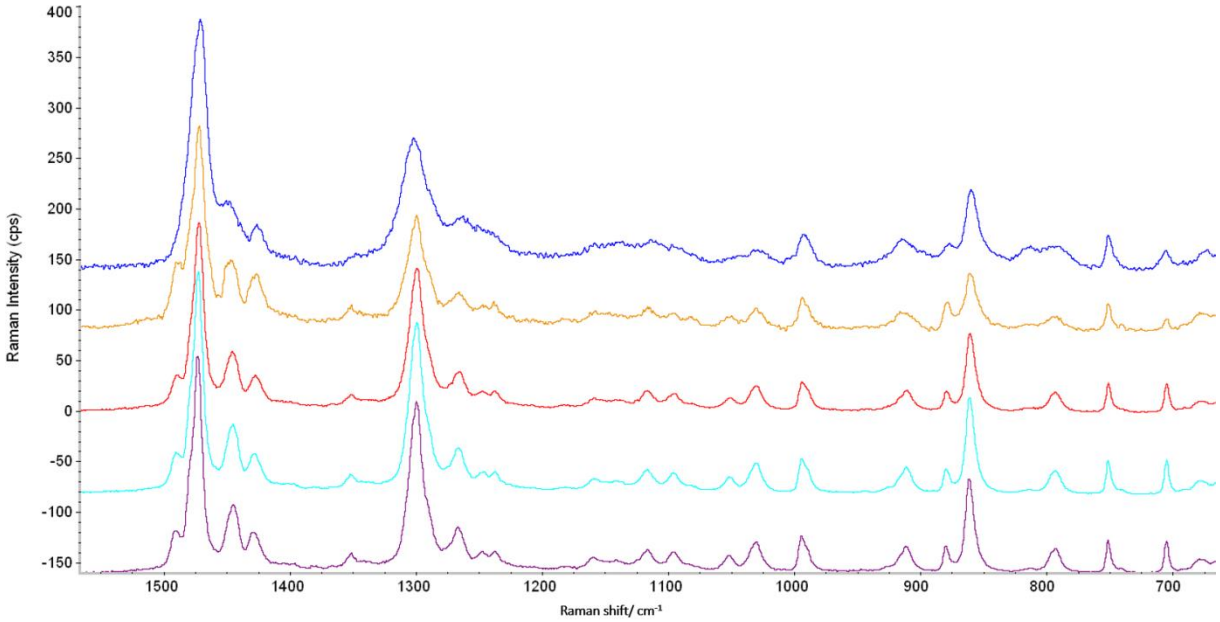

Figure SI-31: Imidazole ring stretching (1500 cm^{-1}- 1200 cm^{-1}), ring bending (~943 cm^{-1}) and CH_2 rocking (900 - 800 cm^{-1}) vibration range in Raman spectra of LiHDI-12C4 solvate in different temperatures: purple - 30 °C, light blue - 50 °C, red - 70 °C, orange - 90 °C (melting started), and blue - 120 °C (melted).

5.2.2 In 15C5 crown ether

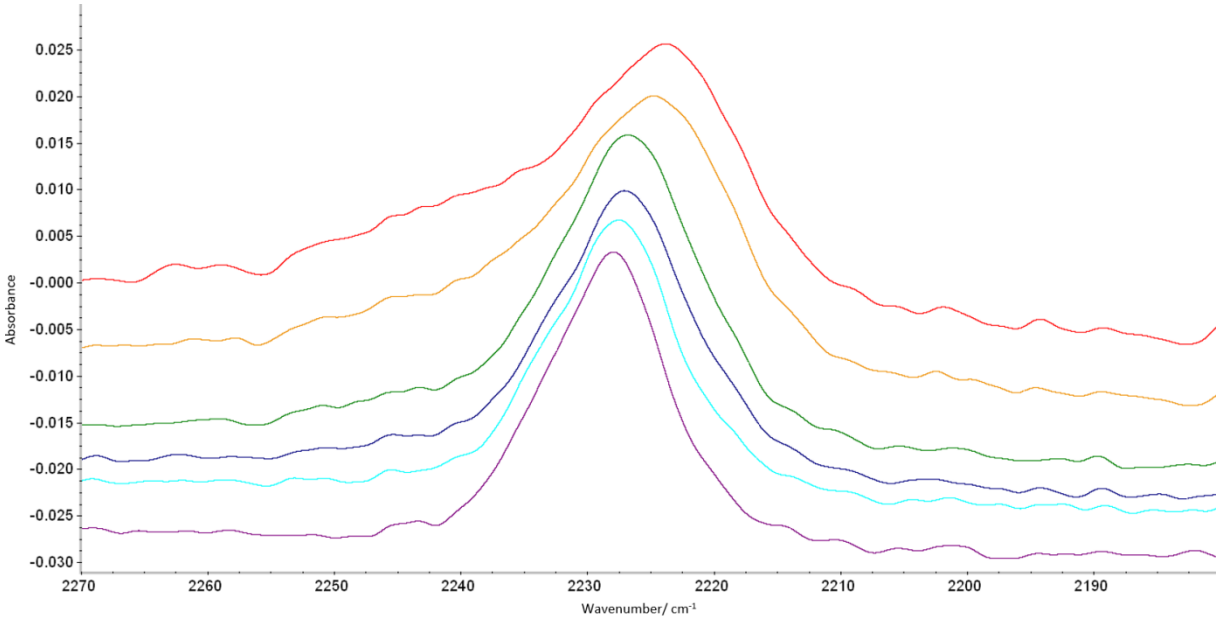

Figure SI-32: CN stretching vibration range in spectra of LiHDI-15C5 solvate in different temperatures: purple - 30 °C, light blue - 50 °C, blue - 70 °C , green - 80 °C (solution), yellow - 80 °C (crystal), and red - 110 °C.

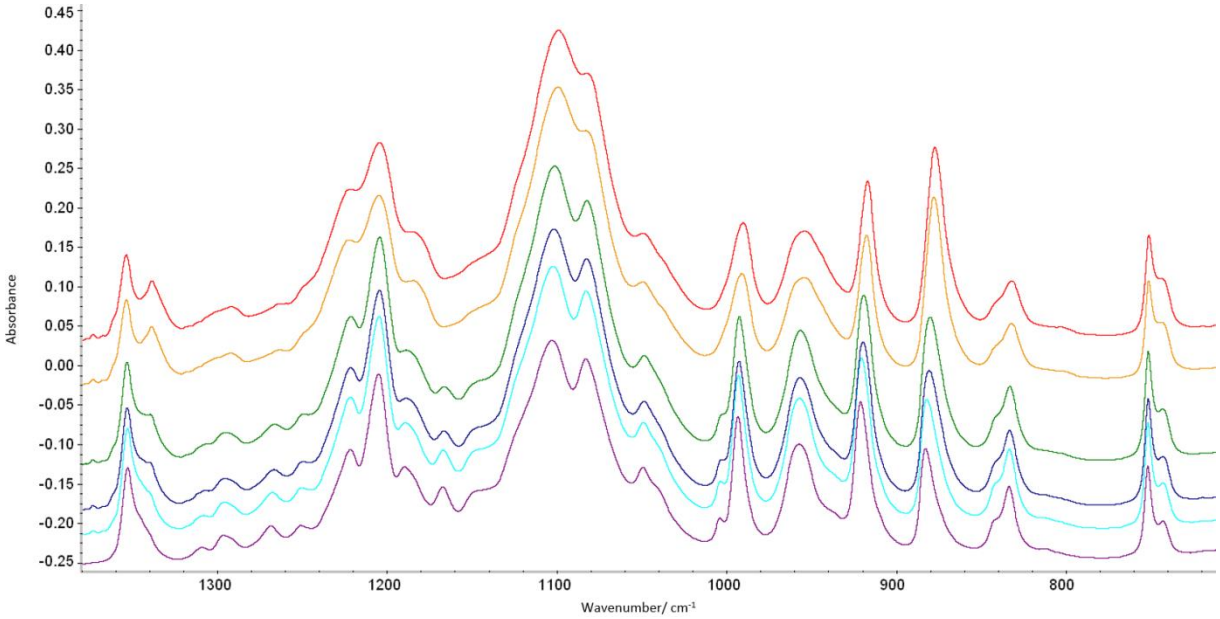

Figure SI-33: Imidazole ring bending (~1000 cm^{-1}), C-O stretching and CH_2 rocking (900 cm^{-1} - 800 cm^{-1}) vibration range in FTIR spectra of LiHDI-15C5 in different temperatures: purple - 30 °C, light blue - 50 °C, blue - 70 °C , green - 80 °C (solution), yellow - 80 °C (crystal), and red - 110 °C.

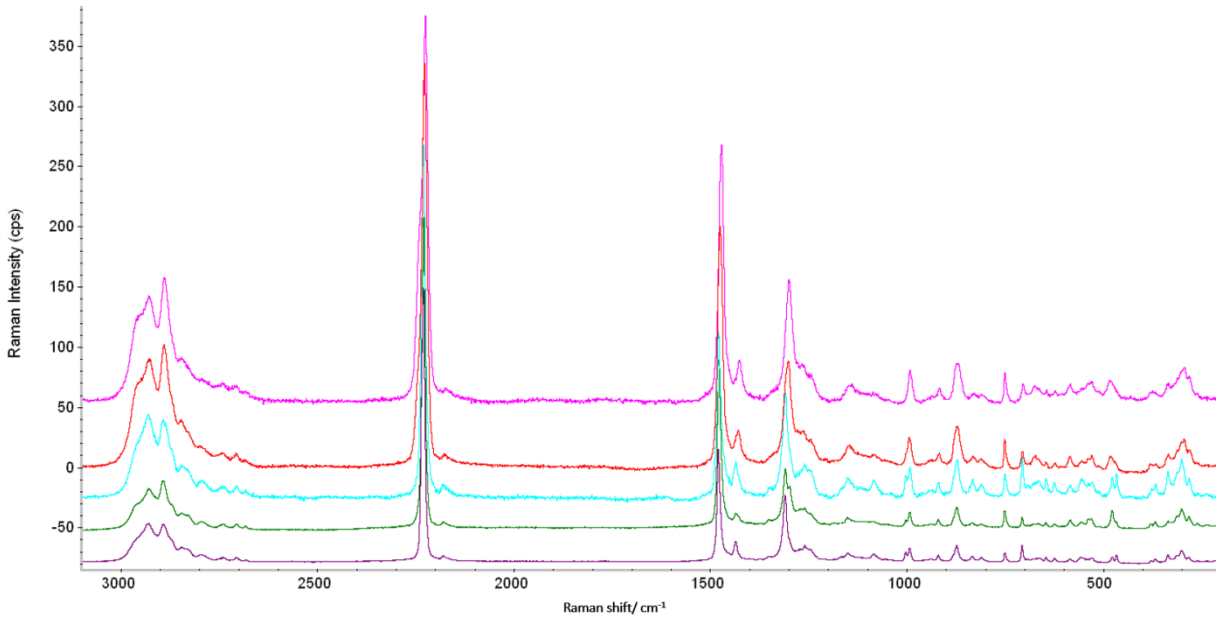

Figure SI-34: Raman spectra of LiHDI-15C5 solvate in different temperatures: purple - 30 °C, green - 50 °C, light blue - 70 °C, red- 80 °C (solution), and pink - 110 °C.

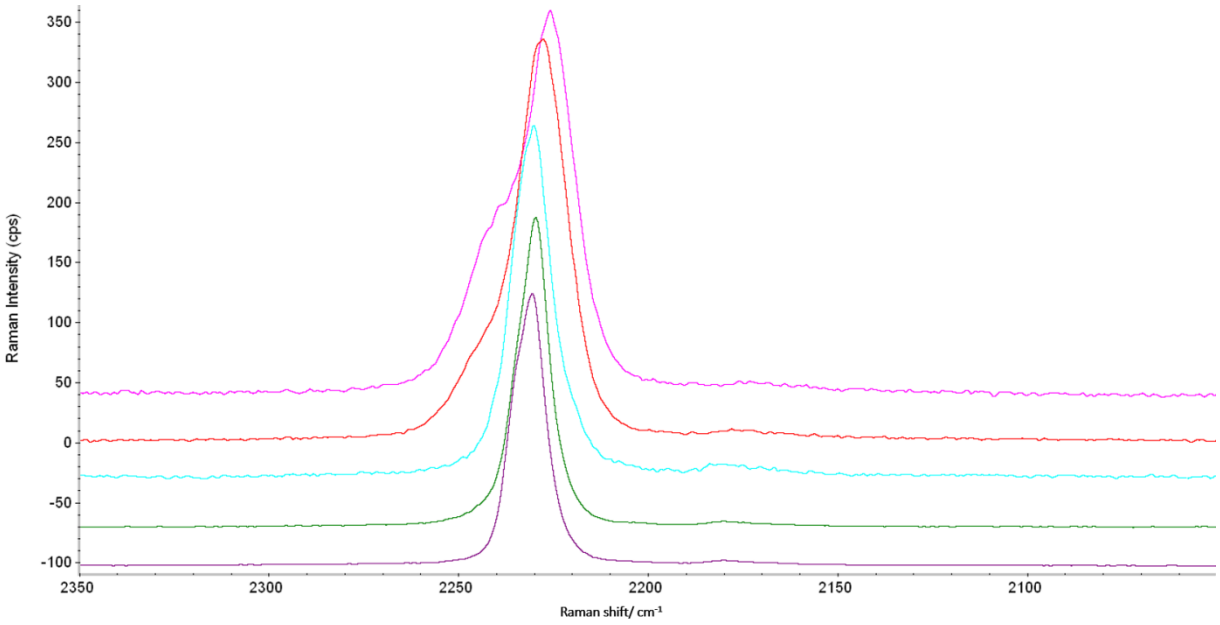

Figure SI-35: CN stretching vibration range in Raman spectra of LiHDI-15C5 in different temperatures: purple - 30 °C, green - 50 °C, light blue - 70 °C, red- 80 °C (solution), and pink - 110 °C.

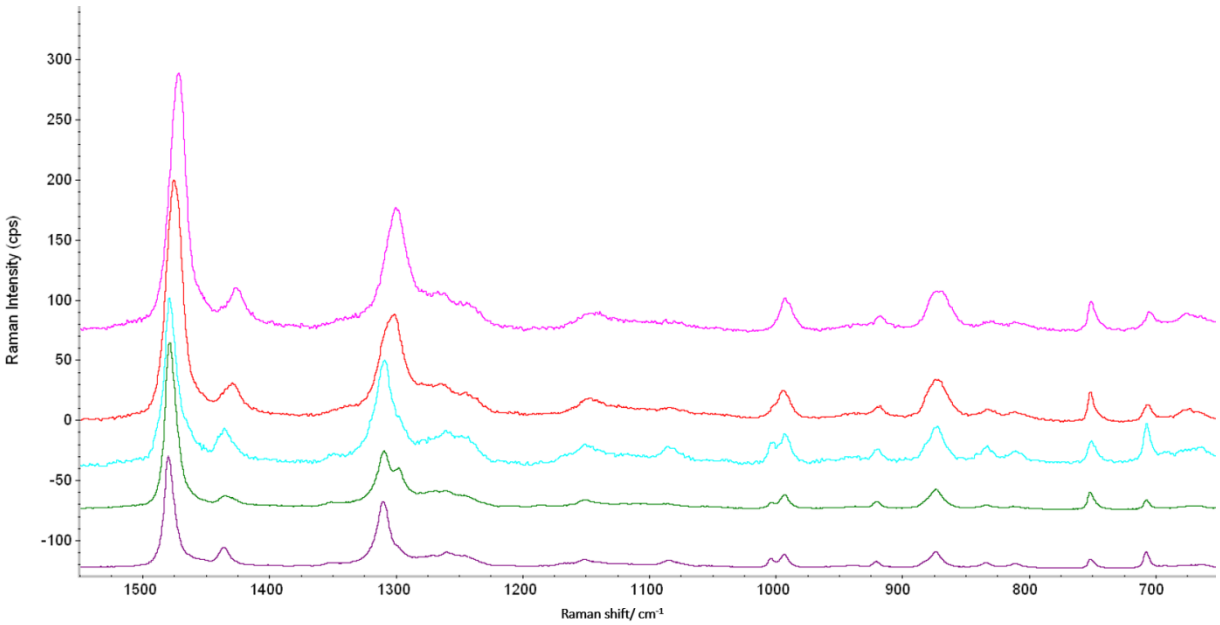

Figure SI-36: Imidazole ring stretching (1500 cm^{-1} - 1200 cm^{-1}), ring bending (~1000 cm^{-1}) and CH_2 rocking (900 cm^{-1} - 800 cm^{-1}) vibration range in Raman spectra of LiHDI-15C5 in different temperatures: purple - 30 °C, green - 50 °C, light blue - 70 °C , red - 80 °C and pink - 110 °C.

References

1 A. Narayanan Krishnamoorthy, C. Wölke, D. Diddens, M. Maiti, Y. Mabrouk, P. Yan, M. Grünebaum, M. Winter, A. Heuer and I. Cekic-Laskovic, Data-Driven Analysis of High-Throughput Experiments on Liquid Battery Electrolyte Formulations: Unraveling the Impact of Composition on Conductivity, *Chemistry–Methods*, 2022, **2**, 1–8.

2 L. Niedzicki, G. Z. Żukowska, M. Bukowska, P. Szczeciński, S. Grugeon, S. Laruelle, M. Armand, S. Panero, B. Scrosati, M. Marcinek and W. Wieczorek, New type of imidazole based salts designed specifically for lithium ion batteries, *Electrochimica Acta*, 2010, **55**, 1450–1454.